Inorganic Chemistry

Article

pubs.acs.org/IC

The Redox Chemistry of $[Co_6C(CO)_{15}]^{2-}$: A Synthetic Route to New Co-Carbide Carbonyl Clusters

Iacopo Ciabatti,[†] Cristina Femoni,[†] Mohammad Hayatifar,[†] Maria Carmela Iapalucci,[†] Giuliano Longoni,[†] Calogero Pinzino,[‡] Matilde Valeria Solmi,[†] and Stefano Zacchini*[,†]

[†]Dipartimento di Chimica Industriale "Toso Montanari", Università di Bologna, Viale Risorgimento 4 - 40136 Bologna, Italy

[‡]Area della Ricerca, ICCOM-CNR UOS Pisa, Via G. Moruzzi 1, 56124 Pisa, Italy

Supporting Information

ABSTRACT: The oxidation and reduction reactions of $[Co_6C(CO)_{15}]^{2-}$ have been studied in detail, leading to the isolation of several new Co-carbide carbonyl clusters. Thus, $[Co_6C(CO)_{15}]^{2-}$ reacts in tetrahydrofuran (THF) with oxidants such as $HBF_4{\cdot}Et_2O$ and $[Cp_2Fe][PF_6]$, resulting first in the formation of the previously reported $[Co_6C(CO)_{14}]^-$; then, in CH_2Cl_2, the new dicarbide $[Co_{11}C_2(CO)_{23}]^{2-}$ is formed. The latter may be further oxidized, yielding the isostructural monoanion $[Co_{11}C_2(CO)_{23}]^-$, whereas its reduction with $(cyclopentadienyl)_2Co$ affords the unstable trianion $[Co_{11}C_2(CO)_{23}]^{3-}$, which decomposes during workup. Oxidation of $[Co_6C(CO)_{15}]^{2-}$ in CH_3CN with $[C_7H_7][BF_4]$ affords the same major products, and besides, the new monoacetylide $[Co_{10}(C_2)(CO)_{21}]^{2-}$ was obtained as side-product. Conversely, the reduction of $[Co_6C(CO)_{15}]^{2-}$ in THF with increasing amounts of Na/naphthalene results in the following species: $[Co_6C(CO)_{13}]^{2-}$, $[Co_{11}(C_2)(CO)_{22}]^{3-}$, $[Co_7C(CO)_{15}]^{3-}$, $[Co_8C(CO)_{17}]^{4-}$, $[Co_6C(CO)_{12}]^{3-}$, and $[Co(CO)_4]^-$. The new $[Co_{11}C_2(CO)_{23}]^-$, $[Co_{11}C_2(CO)_{23}]^{2-}$, $[Co_{10}(C_2)(CO)_{21}]^{2-}$, $[Co_8C(CO)_{17}]^{4-}$, $[Co_6C(CO)_{12}]^{3-}$, and $[Co_7C(CO)_{15}]^{3-}$ clusters were structurally characterized. Moreover, the paramagnetic species $[Co_{11}C_2(CO)_{23}]^{2-}$ and $[Co_6C(CO)_{12}]^{3-}$ were investigated by means of electron paramagnetic resonance spectroscopy. Finally, electrochemical studies were performed on $[Co_{11}C_2(CO)_{23}]^{n-}$ (n = 1–3).

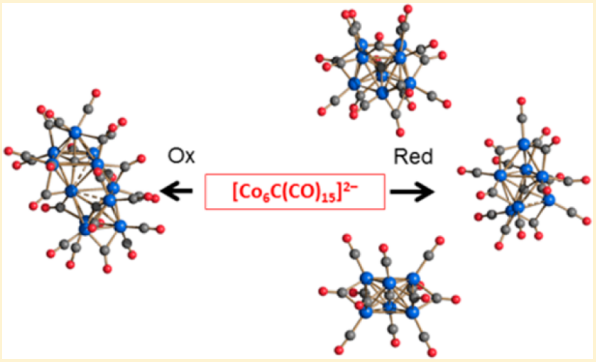

1. INTRODUCTION

The trigonal prismatic $[Co_6C(CO)_{15}]^{2-}$ monocarbido carbonyl cluster has been known for nearly 40 years and has played an important role in the development of the chemistry of metal carbonyl clusters.[1] Meanwhile, other Co-carbonyl clusters containing one interstitial carbide atom have been characterized, that is, the octahedral $[Co_6C(CO)_{13}]^{2-}$ and $[Co_6C(CO)_{14}]^-$, and the square antiprismatic $[Co_8C(CO)_{18}]^{2-}$.[2,3] In addition, the dicarbide $[Co_{13}C_2(CO)_{24}]^{n-}$ (n = 3,4) and the monoacetylides $[Co_9(C_2)(CO)_{19}]^{2-}$ and $[Co_{11}(C_2)(CO)_{22}]^{3-}$ have been reported.[4−6] Most of these Co-carbide clusters may be obtained directly from $[Co_6C(CO)_{15}]^{2-}$ by chemical or thermal methods, even if sometimes alternative syntheses are more convenient. The rich chemistry of molecular Co-carbonyl carbides should be contrasted with the fact that carbon is almost insoluble in bulk Co. Indeed, only two metastable Co–C phases are known in the bulk, that is, Co_3C and Co_2C.[7]

Molecular Co-carbide carbonyl clusters are interesting because of their structural, chemical, and physical properties. The presence of interstitial carbide atoms contributes to an extra stabilization of these clusters compared to homometallic species,[8] leading to higher nuclearity clusters. For instance, the largest homometallic Co-carbonyl is $[Co_6(CO)_{15}]^{2-}$,[9] whereas a nuclearity of 13 may be reached by introducing interstitial C-atoms. Because of this enhanced stability, molecular Co-carbide clusters may also undergo more easily to reversible redox processes and/or exist as paramagnetic odd electron species. For instance, both $[Co_8C(CO)_{18}]^{2-}$ and $[Co_{13}C_2(CO)_{24}]^{3-}$ reveal a rich redox propensity, including several reversible processes in the time scale of cyclic voltammetry.[2,3] Moreover, the $[Co_6C(CO)_{14}]^-$, $[Co_9(C_2)(CO)_{19}]^{2-}$, and $[Co_{13}C_2(CO)_{24}]^{4-}$ monoradicals have been isolated and structurally characterized.[2,4] The structures of all these Co-carbide carbonyl clusters seem to be the result of the balance among Co–Co, Co-CO, and Co–$C_{carbide}$ (sometimes also C–C) interactions, as well as the formation of suitable cavities to lodge the carbide atoms.[8,10] It is noteworthy that recent work on metal-catalyzed formation of carbon structures, for example, fullerenes and carbon nanotubes, may likely depend on how C-fragments are stabilized and joined on a metal framework.[11−13] Thus, the study of molecular carbide clusters may contribute also to these current topics.[10]

Electrochemical studies of $[Co_6C(CO)_{15}]^{2-}$ indicate that this species undergoes two one-electron oxidations, leading to the quite unstable monoanion and neutral congeners, respectively

Received: January 22, 2014
Published: March 21, 2014

   dx.doi.org/10.1021/ic500161e | Inorg. Chem. 2014, 53, 3818–3831

($E_{p2-/-}$ = 0.00 V; $E_{p-/0}$ = +0.15 V; all potentials are referenced to saturated calomel electrode (SCE)).[14] In accordance with the chemical oxidation, exhaustive electrolysis in correspondence to the most anodic process affords, among different oxidation products, the partially decarbonylated $[Co_6C(CO)_{14}]^-$.[14] Moreover, $[Co_6C(CO)_{15}]^{2-}$ also undergoes a two-electron reduction at E_p = −1.75 V, irreversible in character. These electrochemical data suggest that redox reactions might be used to convert $[Co_6C(CO)_{15}]^{2-}$ into new carbide clusters. Nonetheless, up to now the only product isolated in this way was $[Co_6C(CO)_{14}]^-$, obtained by the mild oxidation of $[Co_6C(CO)_{15}]^{2-}$. In addition, it was reported that the reaction of $[Co_6C(CO)_{15}]^{2-}$ with an excess of Na/naphthalene results in its decomposition to $[Co(CO)_4]^-$.

Thus, we decided to reinvestigate the redox reactions of $[Co_6C(CO)_{15}]^{2-}$, and our results are summarized in this Paper. We will describe first its oxidation reactions, which lead to the new $[Co_{11}C_2(CO)_{23}]^{n-}$ (n = 1−3) and $[Co_{10}(C_2)(CO)_{21}]^{2-}$ clusters, and then the reduction of $[Co_6C(CO)_{15}]^{2-}$, which affords mixtures of products, among which the new $[Co_7C(CO)_{15}]^{3-}$, $[Co_8C(CO)_{17}]^{4-}$, and $[Co_6C(CO)_{12}]^{3-}$ species have been isolated. All the new clusters were structurally characterized, and in addition, electron paramagnetic resonance (EPR) studies were carried out on the paramagnetic $[Co_{11}C_2(CO)_{23}]^{2-}$ and $[Co_6C(CO)_{12}]^{3-}$ species.

2. RESULTS AND DISCUSSION

2.1. Oxidation of $[Co_6C(CO)_{15}]^{2-}$: Synthesis, Spectroscopic, and Electrochemical Characterization of $[Co_{11}C_2(CO)_{23}]^{n-}$ (n = 1−3). $[Co_6C(CO)_{15}]^{2-}$ is readily oxidized in tetrahydrofuran (THF) by miscellaneous oxidants such as $HBF_4{\cdot}Et_2O$ and $[Cp_2Fe][PF_6]$ (Cp = cyclopentadienyl), resulting in the formation of the previously reported $[Co_6C(CO)_{14}]^-$ (eq 1).[2,3] The nature of this cluster has been determined via IR spectroscopy and confirmed by X-ray crystallography as its $[NMe_3(CH_2Ph)][Co_6C(CO)_{14}]$ and $[NEt_4][Co_6C(CO)_{14}]$ salts.

$$[Co_6C(CO)_{15}]^{2-} + H^+ \rightarrow [Co_6C(CO)_{14}]^- + 0.5H_2 \quad (1)$$

In agreement with eq 1, the reaction requires 1 equiv of oxidant, and apparently (by IR spectroscopy), no further reaction occurs after adding larger amounts of oxidant (2−6 equiv). Nonetheless, further oxidation to give the new dicarbide $[Co_{11}C_2(CO)_{23}]^{2-}$ was observed after removing the THF in vacuo and dissolving the residue in CH_2Cl_2. Complete formation of $[Co_{11}C_2(CO)_{23}]^{2-}$ requires 3−4 equiv of $HBF_4{\cdot}Et_2O$, whereas a larger amount of $[Cp_2Fe][PF_6]$ (4−6 equiv) is needed. Conversion of $[Co_6C(CO)_{14}]^-$ into $[Co_{11}C_2(CO)_{23}]^{2-}$ may be explained on the basis of eqs 2 and 3, even if the reactions are completed only after the addition of larger amounts of oxidizing agent compared to the stoichiometric ones.

$$2[Co_6C(CO)_{14}]^- + 2H^+ \rightarrow [Co_{11}C_2(CO)_{23}]^{2-} + Co^{2+} + 5CO + H_2 \quad (2)$$

$$2[Co_6C(CO)_{14}]^- + 2[Cp_2Fe]^+ \rightarrow [Co_{11}C_2(CO)_{23}]^{2-} + Co^{2+} + 5CO + 2Cp_2Fe \quad (3)$$

Similarly, the transformation of $[Co_6C(CO)_{15}]^{2-}$ into $[Co_{11}C_2(CO)_{23}]^{2-}$ is described by eq 4, when $HBF_4{\cdot}Et_2O$ is employed.

$$2[Co_6C(CO)_{15}]^{2-} + 4H^+ \rightarrow [Co_{11}C_2(CO)_{23}]^{2-} + Co^{2+} + 7CO + 2H_2 \quad (4)$$

Previous electrochemical studies (summarized in the Introduction) have shown that $[Co_6C(CO)_{15}]^{2-}$ undergoes two one-electron oxidations at E_p = 0.00 and E_p = +0.15 V.[14] Therefore, very mild conditions are required to remove the first electron, affording an unstable monoanion that readily loses CO, resulting in the formation of $[Co_6C(CO)_{14}]^-$. Moreover, the second oxidation process occurs at a very similar potential, suggesting that the same oxidant might promote both reactions, depending on its standard potential, the stoichiometry, and/or solvent. Thus, we can conclude that the two irreversible oxidations observed in the electrochemistry of $[Co_6C(CO)_{15}]^{2-}$ correspond to the subsequent reactions eq 1 and eq 2, which lead to $[Co_6C(CO)_{14}]^-$ and $[Co_{11}C_2(CO)_{23}]^{2-}$. The molecular structure of the $[Co_{11}C_2(CO)_{23}]^{2-}$ dianion was determined as three different salts, that is, $[NMe_3(CH_2Ph)]_2[Co_{11}C_2(CO)_{23}]$, $[NMe_3(CH_2Ph)]_2[Co_{11}C_2(CO)_{23}]{\cdot}0.25CH_2Cl_2$, and $[NEt_4]_2[Co_{11}C_2(CO)_{23}]$ (Section 2.3 and Experimental Section).

Crystals of $[NMe_3(CH_2Ph)]_2[Co_{11}C_2(CO)_{23}]$ display ν(CO) stretchings at 2012(vs), 1852(m) cm^{-1} in nujol mull and at 2018(vs), 1853(ms) cm^{-1} in CH_2Cl_2 solution. The paramagnetic nature of $[NMe_3(CH_2Ph)]_2[Co_{11}C_2(CO)_{23}]$ was confirmed by EPR studies. Thus, the EPR spectrum recorded on a solid sample of $[NMe_3(CH_2Ph)]_2[Co_{11}C_2(CO)_{23}]$ shows already at 298 K (Figure 1) a strong signal attributable to an S = 1/2 system with g_1 = 2.057 30, g_2 = 2.047 73, and g_3 = 2.034 52 [line width used for simulation ΔH_1 = 141.66 G, ΔH_2 = 223.89 G, and ΔH_3 = 49.92 G]. The presence of one unpaired electron per cluster is confirmed also by the EPR spectrum recorded in CH_2Cl_2 solution at 193 K, which shows an isotropic signal with g_{iso} = 2.035 29 and ΔH = 103.2 G (Figure 2). For comparison, the paramagnetic $[Co_{13}C_2(CO)_{24}]^{4-}$ displays in the solid state at 123 K one EPR signal due to one unpaired electron with g = 2.13 and ΔH = 300 G.[4] Density functional theory (DFT) calculations on $[Co_{11}C_2(CO)_{23}]^{2-}$ (see Experimental Section for details) show that the unpaired electron is mainly delocalized on the $Co_{11}C_2$ cage of the cluster (Figure 3).

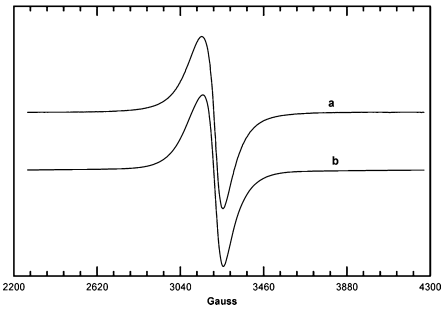

Figure 1. X-band EPR spectrum of $[NMe_3(CH_2Ph)]_2[Co_{11}C_2(CO)_{23}]$ as solid registered at 298 K. (a) Experimental. (b) Simulation.

Electrochemical studies of $[Co_{11}C_2(CO)_{23}]^{2-}$ in THF solution show that this dianion undergoes a one-electron oxidation ($E^{\circ\prime}_{-/2-}$ = +0.01 V) and a one-electron reduction

dx.doi.org/10.1021/ic500161e | Inorg. Chem. 2014, 53, 3818−3831

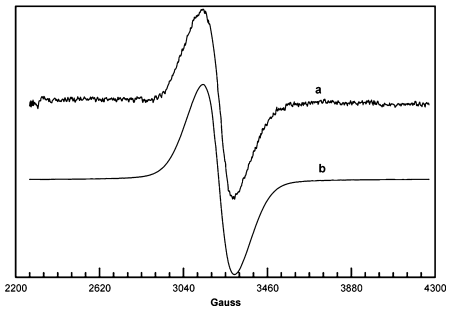

Figure 2. X-band EPR spectrum of $[NMe_3(CH_2Ph)]_2[Co_{11}C_2(CO)_{23}]$ in CH_2Cl_2 solution registered at 193 K. (a) Experimental. (b) Simulation.

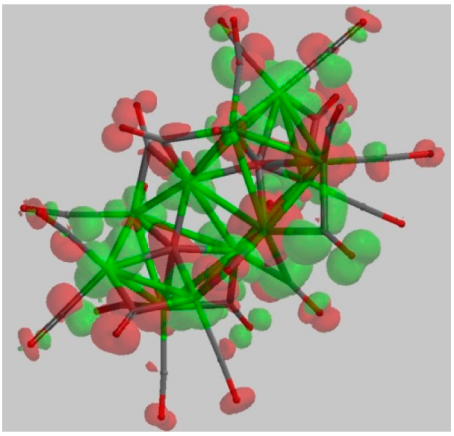

Figure 3. DFT calculated spin density surface (0.002 electron/au^3) of the $[Co_{11}C_2(CO)_{23}]^{2-}$ cluster (red, negative spin density; green, positive spin density).

($E^{\circ\prime}_{2-/3-}$ = −0.63 V), both with features of chemical reversibility (Figure 4) attributable to the $[Co_{11}C_2(CO)_{23}]^{n-}$ (n = 1−3) species.

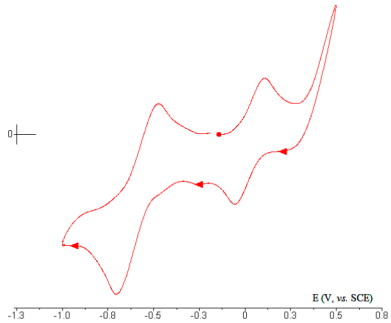

Figure 4. Cyclic voltammogram recorded at a gold electrode in THF of $[NMe_3(CH_2Ph)]_2[Co_{11}C_2(CO)_{23}]$ (2.0×10^{-3} M). $[NBu_4][BF_4]$ (0.1 M) supporting electrolyte. Scan rate = 0.1 V s^{-1}.

In view of this electrochemical behavior, we attempted to perform the same redox reactions also by chemical methods. Oxidation of $[Co_{11}C_2(CO)_{23}]^{2-}$ to give $[Co_{11}C_2(CO)_{23}]^{-}$ can be easily accomplished by adding $HBF_4{\cdot}Et_2O$ to its CH_2Cl_2 solution, in agreement with eq 5.

$$[Co_{11}C_2(CO)_{23}]^{2-} + H^+ \rightarrow [Co_{11}C_2(CO)_{23}]^{-} + 0.5H_2 \quad (5)$$

The monoanion is very stable, and crystals suitable for X-ray analyses of $[NMe_3(CH_2Ph)][Co_{11}C_2(CO)_{23}]$ and $[NMe_3(CH_2Ph)][Co_{11}C_2(CO)_{23}]{\cdot}0.5CH_2Cl_2$ were obtained by slow diffusion of n-hexane into the crystal/CH_2Cl_2 solution. The same compound may be obtained directly from $[Co_6C(CO)_{15}]^{2-}$ by adding a large excess (6−8 equiv) of $HBF_4{\cdot}Et_2O$ to its THF solution, removing the solvent in vacuo, and dissolving the residue in CH_2Cl_2 (eq 6). Crystals of $[NMe_3(CH_2Ph)][Co_{11}C_2(CO)_{23}]$ display ν(CO) stretchings at 2030(vs), 1874(m) cm^{-1} in nujol mull and at 2050(vs), 1876(ms) cm^{-1} in CH_2Cl_2 solution.

$$2[Co_6C(CO)_{15}]^{2-} + 5H^+ \rightarrow [Co_{11}C_2(CO)_{23}]^{-} + Co^{2+} + 7CO + 2.5H_2 \quad (6)$$

In view of the potential measured for the reduction of $[Co_{11}C_2(CO)_{23}]^{2-}$ to $[Co_{11}C_2(CO)_{23}]^{3-}$ ($E^{\circ\prime}_{2-/3-}$ = −0.63 V), we used Cp_2Co ($E^{\circ\prime}$ = −0.90 V) as reducing agent. Indeed, after the addition of 1 equiv of Cp_2Co to a THF solution of $[Co_{11}C_2(CO)_{23}]^{2-}$ its carbonyl stretchings are lowered to ν(CO) 1976 (vs), 1768(m) cm^{-1}, in agreement with the formation of a hypothetical $[Co_{11}C_2(CO)_{23}]^{3-}$ trianion (eq 7). For comparison, the previously reported monoacetylide $[Co_{11}(C_2)(CO)_{22}]^{3-}$ displays ν(CO) at 1974 (vs), 1800(m) cm^{-1}.[6]

$$[Co_{11}C_2(CO)_{23}]^{2-} + Cp_2Co \rightarrow [Co_{11}C_2(CO)_{23}]^{3-} + [Cp_2Co]^+ \quad (7)$$

Unfortunately, this species is not stable enough to be isolated and fully characterized. All attempts to obtain it in a crystalline form failed, resulting instead in crystals of $[Cp_2Co]_2[Co_6C(CO_{15}]$ or $[NMe_3(CH_2Ph)]_2[Co_6C(CO)_{15}]$. The tentative formulation of the reduced species as $[Co_{11}C_2(CO)_{23}]^{3-}$ is based on the above IR and electrochemical data.

Finally, we investigated the oxidation of $[Co_6C(CO)_{15}]^{2-}$ with $[C_7H_7]^+$, resulting in $[Co_6C(CO)_{14}]^{-}$ and $[Co_{11}C_2(CO)_{23}]^{2-}$ as the major products. Nonetheless, during workup (see Experimental Section), it was possible to obtain as a side product the new monoacetylide $[Co_{10}(C_2)(CO)_{21}]^{2-}$, which was structurally characterized as its $[NMe_3(CH_2Ph)]_2[Co_{10}(C_2)(CO)_{21}]$ salt. These crystals show ν(CO) stretchings at 1997(vs), 1976(m), 1957(sh), 1935(m), 1887(m), 1844(ms), and 1879(m) cm^{-1} in nujol mull and 2010(vs), 1833(ms) cm^{-1} in CH_2Cl_2 solution. The dianion $[Co_{10}(C_2)(CO)_{21}]^{2-}$ was obtained as a byproduct in very low yields, and thus, no further characterization was performed.

2.2. Reduction of $[Co_6C(CO)_{15}]^{2-}$: Synthesis and Characterization of $[Co_6C(CO)_{12}]^{3-}$, $[Co_7C(CO)_{15}]^{3-}$, and $[Co_8C(CO)_{17}]^{4-}$. It has been determined by electrochemistry that $[Co_6C(CO)_{15}]^{2-}$ undergoes an irreversible two-electron reduction at E_p = −1.75 V.[14] In agreement with this observation, $[Co_6C(CO)_{15}]^{2-}$ does not react with Cp_2Co ($E^{\circ\prime}$ = −0.90 V), even in large excess. Thus a stronger reducing agent, such as Na/naphthalene in THF ($E^{\circ\prime}$ = −2.54 V),[15] must be used. Indeed, the reaction of $[Co_6C(CO)_{15}]^{2-}$ with Na/naphthalene in THF affords mixtures of different products, whose nature depends on the amount of reducing agent employed. Most of these compounds have been spectroscopically identified and partially separated, owing to their differential solubility in organic solvents. The species so far identified include some compounds that were already known, that is, $[Co(CO)_4]^{-}$, $[Co_6C(CO)_{13}]^{2-}$, and $[Co_{11}(C_2)$-

dx.doi.org/10.1021/ic500161e | Inorg. Chem. 2014, 53, 3818−3831

$(CO)_{22}]^{3-}$,[2,6,16] as well as the new clusters $[Co_8C(CO)_{17}]^{4-}$, $[Co_7C(CO)_{15}]^{3-}$, and $[Co_6C(CO)_{12}]^{3-}$. All the new species were structurally characterized by means of X-ray crystallography, whereas the other compounds were spectroscopically identified.

As a general procedure, $[Co_6C(CO)_{15}]^{2-}$ was treated with increasing amounts of Na/naphthalene in THF, and then the solvent was removed in vacuo. The residue was dissolved in dimethylformamide (DMF) and treated with an excess of an aqueous solution of $[NMe_3(CH_2Ph)]Cl$ or $[NEt_4]Br$ to exchange Na^+ with a tetra-alkylammonium cation. The obtained solid was recovered by filtration, washed with H_2O and toluene, and then extracted with organic solvents of increasing polarity (THF, acetone, CH_3CN, DMF). This resulted in crystals of $[NEt_4]_3[Co_{11}(C_2)(CO)_{22}]\cdot 2CH_3COCH_3$, $[NMe_3(CH_2Ph)]_4[Co_8C(CO)_{17}]$, $[NMe_3(CH_2Ph)]_3[Co_6C(CO)_{12}]\cdot 4CH_3CN$, and $[NEt_4]_3[Co_7C(CO)_{15}]$ that were suitable for X-ray analyses (see Experimental Section for details).

The first product of the reaction of $[Co_6C(CO)_{15}]^{2-}$ with Na/naphthalene is $[Co_6C(CO)_{13}]^{2-}$, which, actually, is a decarbonylation and not a reduction product (eq 8). Decarbonylation is likely to be promoted by the reducing agent.[17] Further decarbonylation with concomitant elimination of $[Co(CO)_4]^-$ results in $[Co_{11}(C_2)(CO)_{22}]^{3-}$ (eq 9). Then, after adding larger amounts of Na/naphthalene, the three new reduced species $[Co_7C(CO)_{15}]^{3-}$, $[Co_8C(CO)_{17}]^{4-}$, and $[Co_6C(CO)_{12}]^{3-}$ are sequentially formed, in agreement with the reactions given in eqs 10, 11, and 12. The $[Co(CO)_4]^-$ anion is formed as a side product of the reactions given in eqs 9−12 and, in addition, is also the final product of reduction, in agreement with eq 13, as previously reported. (The CO required by eq 13 is generated as described by eqs 8−12.)

$$[Co_6C(CO)_{15}]^{2-} \rightarrow [Co_6C(CO)_{13}]^{2-} + 2CO \quad (8)$$

$$2[Co_6C(CO)_{15}]^{2-} \rightarrow [Co_{11}(C_2)(CO)_{22}]^{3-} + [Co(CO)_4]^- + 4CO \quad (9)$$

$$2[Co_6C(CO)_{15}]^{2-} + 2Na \rightarrow [Co_7C(CO)_{15}]^{3-} + 3[Co(CO)_4]^- + 2Co + C + 3CO + 2Na^+ \quad (10)$$

$$2[Co_6C(CO)_{15}]^{2-} + 3Na \rightarrow [Co_8C(CO)_{17}]^{4-} + 3[Co(CO)_4]^- + Co + C + CO + 3Na^+ \quad (11)$$

$$2[Co_6C(CO)_{15}]^{2-} + 3Na \rightarrow [Co_6C(CO)_{12}]^{3-} + 4[Co(CO)_4]^- + 2Co + 2CO + 3Na^+ \quad (12)$$

$$[Co_6C(CO)_{15}]^{2-} + 4Na + 9CO \rightarrow 6[Co(CO)_4]^- + C + 4Na^+ \quad (13)$$

Overall, as summarized in Scheme 1, the different products are formed in the following sequence: $[Co_6C(CO)_{13}]^{2-}$, $[Co_{11}(C_2)(CO)_{22}]^{3-}$, $[Co_7C(CO)_{15}]^{3-}$, $[Co_8C(CO)_{17}]^{4-}$, $[Co_6C(CO)_{12}]^{3-}$, and $[Co(CO)_4]^-$. This corresponds to a gradual decrease of the oxidation state of cobalt from −0.33 to −1 (Table 1), apart from $[Co_{11}(C_2)(CO)_{22}]^{3-}$ (−0.18), which is actually more oxidized and is formed by the disproportionation reaction (eq 9) together with the more reduced species $[Co(CO)_4]^-$ (−1).

Scheme 1

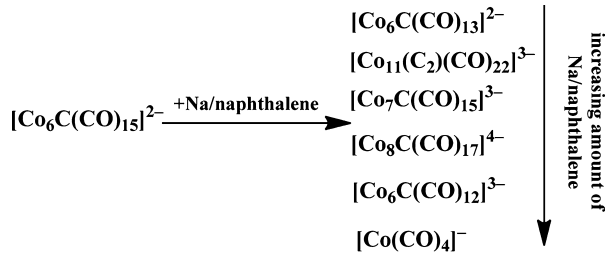

Table 1. IR Data, Oxidation State (Charge/M), and CO/M Ratio for the Different Co-Carbide Carbonyl Clusters

	charge/M[a]	CO/M	ν(t-CO)	ν(μ-CO)
$[Co_{11}C_2(CO)_{23}]^-$	−0.09	2.09	2050	1876
$[Co_6C(CO)_{14}]^-$	−0.17	2.33	2012	1855
$[Co_{11}C_2(CO)_{23}]^{2-}$	−0.18	2.09	2018	1853
$[Co_{10}(C_2)(CO)_{21}]^{2-}$	−0.20	2.10	2007	1837
$[Co_9(C_2)(CO)_{19}]^{2-}$	−0.22	2.11	1989	1832
$[Co_{13}C_2(CO)_{24}]^{3-}$	−0.23	1.85	1990	1812, 1782
$[Co_8C(CO)_{18}]^{2-}$	−0.25	2.25	1993	1813
$[Co_{11}C_2(CO)_{23}]^{3-}$	−0.27	2.09	1976	1768
$[Co_{11}(C_2)(CO)_{22}]^{3-}$	−0.27	2	1974	1800
$[Co_{13}C_2(CO)_{24}]^{4-}$	−0.31	1.85	1960	1785, 1758
$[Co_6C(CO)_{15}]^{2-}$	−0.33	2.5	1982	1828, 1816
$[Co_6C(CO)_{13}]^{2-}$	−0.33	2.17	1968	1816
$[Co_7C(CO)_{15}]^{3-}$	−0.43	2.14	1943	1770
$[Co_8C(CO)_{17}]^{4-}$	−0.5	2.12	1922	1744
$[Co_6C(CO)_{12}]^{3-}$	−0.5	2	1910	1769
$[Co(CO)_4]^-$	−1	4	1889	

[a]The charge/M ratio (M = number of Co atom in the cluster) coincides with the oxidation state of Co, assuming CO as a neutral ligand and C in zero oxidation state.

The IR data of all the Co-carbide carbonyl clusters known to date (including the new ones characterized in this work) are reported in Table 1, where they are listed in order of increasing negative oxidation state of cobalt (given as charge/M ratio), together with the CO/M ratio. Starting from $[Co_6C(CO)_{15}]^{2-}$, which is in the middle of the list, all the more oxidized species may be obtained by chemical oxidation ($[Co_6C(CO)_{14}]^-$,[2] $[Co_{11}C_2(CO)_{23}]^{2-}$, $[Co_{11}C_2(CO)_{23}]^-$, $[Co_{10}(C_2)(CO)_{21}]^{2-}$), redox condensation ($[Co_8C(CO)_{18}]^{2-}$)[3], or thermal decomposition ($[Co_{11}(C_2)(CO)_{22}]^{3-}$,[6] $[Co_{13}C_2(CO)_{24}]^{4-}$).[4] Only three clusters, that is, $[Co_{11}C_2(CO)_{23}]^{3-}$, $[Co_{13}C_2(CO)_{24}]^{3-}$,[4] and $[Co_9(C_2)(CO)_{19}]^{2-}$,[5] cannot be obtained directly from $[Co_6C(CO)_{15}]^{2-}$, but they are obtained from the reduction of $[Co_{11}C_2(CO)_{23}]^{2-}$, oxidation of $[Co_{13}C_2(CO)_{24}]^{4-}$, and thermal decomposition of $[Co_6C(CO)_{14}]^-$, respectively. Conversely, all the products listed below $[Co_6C(CO)_{15}]^{2-}$ in Table 1 were obtained from its reduction.

As expected, the IR data reported in Table 1 show an almost monotonic dependence on the oxidation state of cobalt. Thus, the ν(CO) frequencies are lowered as the oxidation state of cobalt becomes more negative. When two clusters have similar oxidation states, the one with lower CO/M ratio displays also lower carbonyl stretching frequencies, in agreement with the

dx.doi.org/10.1021/ic500161e | Inorg. Chem. 2014, 53, 3818−3831

increased π-back-donation. This explains also some apparent incongruities in Table 1. For instance, even if cobalt is slightly more reduced in $[Co_6C(CO)_{15}]^{2-}$ (−0.33) than it is in $[Co_{13}C_2(CO)_{24}]^{4-}$ (−0.31), the former hexanuclear cluster displays ν(CO) bands at higher wave numbers, in view of its larger CO content (CO/M = 2.5) compared to $[Co_{13}C_2(CO)_{24}]^{4-}$ (CO/M = 1.85).

Finally, all the products described in this section are diamagnetic apart from $[Co_6C(CO)_{12}]^{3-}$, which possesses one unpaired electron. The EPR spectrum recorded at 298 K on solid $[NMe_3(CH_2Ph)]_3[Co_6C(CO)_{12}]\cdot 4CH_3CN$ (Figure 5)

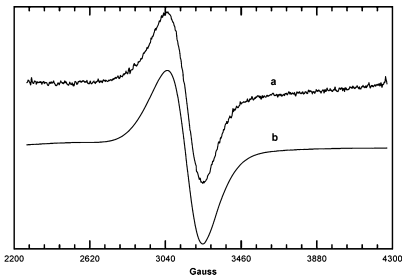

Figure 5. X-band EPR spectrum of $[NMe_3(CH_2Ph)]_3[Co_6C(CO)_{12}]\cdot 4CH_3CN$ as solid registered at 298 K. (a) Experimental. (b) Simulation.

displays a strong signal at g_1 = 2.146 27, g_2 = 2.068 29, and g_3 = 2.038 84 with ΔH_1 = 270.38, ΔH_2 = 119.48, and ΔH_3 = 280.09. Similarly, a signal at g_{iso} = 2.078 45 with ΔH = 101.3 G was recorded in CH_3CN solution at 203 K (Figure 6). DFT calculations indicate that the unpaired electron is delocalized over the Co_6C cage of the cluster (Figure 7).

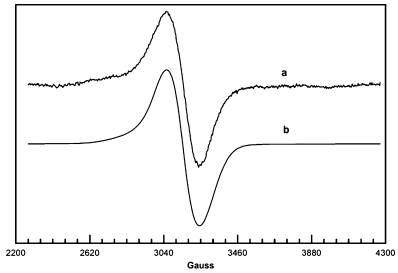

Figure 6. X-band EPR spectrum of $[NMe_3(CH_2Ph)]_3[Co_6C(CO)_{12}]\cdot 4CH_3CN$ in CH_3CN solution registered at 203 K. (a) Experimental. (b) Simulation.

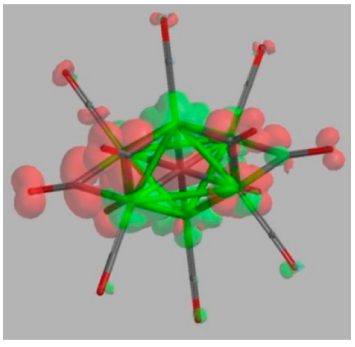

Figure 7. DFT calculated spin density surface (0.002 electron/au^3) of the $[Co_6C(CO)_{12}]^{3-}$ cluster (red, negative spin density; green, positive spin density).

2.3. Crystal Structures of $[Co_{11}C_2(CO)_{23}]^-$, $[Co_{11}C_2(CO)_{23}]^{2-}$, $[Co_{10}(C_2)(CO)_{21}]^{2-}$, $[Co_8C(CO)_{17}]^{4-}$, $[Co_6C(CO)_{12}]^{3-}$, and $[Co_7C(CO)_{15}]^{3-}$.

Crystals structures were determined for the following salts: $[NMe_3(CH_2Ph)][Co_6C(CO)_{14}]$, $[NEt_4][Co_6C(CO)_{14}]$, $[NMe_3(CH_2Ph)]_2[Co_{11}C_2(CO)_{23}]$, $[NMe_3(CH_2Ph)]_2[Co_{11}C_2(CO)_{23}]\cdot 0.25CH_2Cl_2$, $[NEt_4]_2[Co_{11}C_2(CO)_{23}]$, $[NMe_3(CH_2Ph)][Co_{11}C_2(CO)_{23}]$, $[NMe_3(CH_2Ph)][Co_{11}C_2(CO)_{23}]\cdot 0.5CH_2Cl_2$, $[Cp_2Co]_2[Co_6C(CO_{15}]$, $[NMe_3(CH_2Ph)]_2[Co_{10}(C_2)(CO)_{21}]$, $[NEt_4]_3[Co_{11}(C_2)(CO)_{22}]\cdot 2CH_3COCH_3$, $[NMe_3(CH_2Ph)]_4[Co_8C(CO)_{17}]$, $[NMe_3(CH_2Ph)]_3[Co_6C(CO)_{12}]\cdot 4CH_3CN$, and $[NEt_4]_3[Co_7C(CO)_{15}]$. Details are given in the Experimental Section.

In this section, we discuss only the structures of $[NMe_3(CH_2Ph)]_2[Co_{11}C_2(CO)_{23}]$, $[NMe_3(CH_2Ph)][Co_{11}C_2(CO)_{23}]$, $[NMe_3(CH_2Ph)]_2[Co_{10}(C_2)(CO)_{21}]$, $[NMe_3(CH_2Ph)]_4[Co_8C(CO)_{17}]$, $[NMe_3(CH_2Ph)]_3[Co_6C(CO)_{12}]\cdot 4CH_3CN$, and $[NEt_4]_3[Co_7C(CO)_{15}]$, which contain the new clusters $[Co_{11}C_2(CO)_{23}]^{2-}$, $[Co_{11}C_2(CO)_{23}]^-$, $[Co_{10}(C_2)(CO)_{21}]^{2-}$, $[Co_8C(CO)_{17}]^{4-}$, $[Co_6C(CO)_{12}]^{3-}$, and $[Co_7C(CO)_{15}]^{3-}$. Their main bonding parameters are summarized in Table 2. Conversely, all the other salts, which contain these same clusters or species previously reported in the literature as different salts, will not be discussed further. Their CIF files have been deposited within the Cambridge Structural Database for sake of completeness.

$[Co_{11}C_2(CO)_{23}]^{2-}$ and $[Co_{11}C_2(CO)_{23}]^-$. $[Co_{11}C_2(CO)_{23}]^{2-}$ and $[Co_{11}C_2(CO)_{23}]^-$ display very similar structures (Figure 8), since their $Co_{11}C_2$ metal cages (possessing C_2 symmetry) are based on two Co_6C octahedra sharing a common vertex (Figure 9). Three interoctahedra Co−Co bonds are present, in addition to the 24 intraoctahedron Co−Co interactions (12 per each octahedron). Overall, we therefore expect 27 Co−Co bonding interactions. Nonetheless, by considering the covalent radius of Co (1.26 Å)[18] and (arbitrarily) adopting a 20% tolerance, we might consider as Co−Co bonds only interactions shorter than 3.02 Å. In this way, the $[Co_{11}C_2(CO)_{23}]^-$ monoanion contains 25 Co−Co bonds, and the $[Co_{11}C_2(CO)_{23}]^{2-}$ dianion has only 23 bonds. In addition, there are two weakly bonding Co−Co interactions [3.058(7) and 3.249(3) Å] in $[Co_{11}C_2(CO)_{23}]^-$ and four [3.066(3), 3.138(4), 3.238(2), and 3.324(2) Å] in $[Co_{11}C_2(CO)_{23}]^{2-}$. All these elongated contacts are located within the Co_6C octahedra composing the clusters (fragmented lines in Figures 8 and 9). Even if longer than normal Co−Co bonds, these interactions are well below twice the van der Waals radius of Co (4.00 Å), and thus, they might maintain some weak bonding character. It must be remarked that the value of the van der Waals radius of Co is not well-defined.[18]

A similar structure has been previously reported for the $[Co_{11}N_2(CO)_{21}]^{3-}$ dinitride, which was composed by two octahedral Co_6N-units sharing a common vertex.[19] Nonetheless, in the case of the dinitride only two interoctahedra Co−Co bonds were formed, since the two octahedral units were joined with a different angle. Also $[Co_{11}N_2(CO)_{21}]^{3-}$ showed a significant elongation of some Co−Co bonds, and this was explained on the basis of the fact that it is electron rich. Indeed, the cluster possesses 154 cluster valence electrons (CVE), whereas only 150 CVE are expected for an M_{11} cluster composed of two octahedra sharing one vertex and with two additional interoctahedra bonds (86 × 2 (Oh) − 18 (vertex) − 2 × 2 (Oh−Oh bonds) = 150 CVE) (Oh = octahedron).[20]

dx.doi.org/10.1021/ic500161e | Inorg. Chem. 2014, 53, 3818−3831

Table 2. Main Bond Distances (Å) of New Anionic Clusters

	Co−Co[a]	Co−$C_{carbide}$
$[Co_{11}C_2(CO)_{23}]^{2-}$[b]	2.4532(16)−2.8301(15)[c]	1.875(9)−2.032(8)
	average 2.597(8)	average 1.93(3)
$[Co_{11}C_2(CO)_{23}]^{-}$[d]	2.459(3)−2.933(3)[e]	1.874(13)−1.975(13)
	average 2.636(15)	average 1.94(5)
$[Co_{10}(C_2)(CO)_{21}]^{2-}$[f]	2.4691(14)−3.012(2)	1.9038(12)−2.205(3)
	average 2.623(4)	average 2.039(15)[g]
$[Co_8C(CO)_{17}]^{4-}$[h]	2.465615)−2.6690(15)	2.012(7)−2.150(7)
	average 2.527(6)	average 2.07(2)
$[Co_8C(CO)_{18}]^{2-}$[i]	2.464(2)−2.598(2)	1.95(2)−2.20(2)
	average 2.52(8)	average 2.07(6)
$[Co_6C(CO)_{12}]^{3-}$[j]	2.4882(14)−2.820(2)	1.8795(11)−1.8805(11)
	average 2.654(8)	average 1.880(4)
$[Co_6C(CO)_{13}]^{2-}$[k]	2.462(2)−2.926(2)	1.852(4)−1.880(4)
	average 2.639(7)	average 1.867(10)
$[Co_6C(CO)_{14}]^{-}$[l]	2.5252(9)−2.9813(14)	1.881(5)−1.920(4)
	average 2.663(3)	average 1.849(12)
$[Co_7C(CO)_{15}]^{3-}$[m]	2.5022(14)−2.8876(14)[n]	1.870(7)−1.937(7)
	average 2.622(5)	average 1.895(17)

[a]Co−Co bonds have been arbitrarily taken as twice the covalent radius of Co (1.26 Å) with a tolerance of 20% (3.02 Å). [b]As found in $[NMe_3(CH_2Ph)]_2[Co_{11}C_2(CO)_{23}]$. [c]Four further weak Co−Co interactions are present: 3.066(3), 3.138(4), 3.238(2), and 3.324(2) Å. Average (including all Co−Co contacts): 2.614(9) Å. [d]As found in $[NMe_3(CH_2Ph)][Co_{11}C_2(CO)_{23}]$. [e]Two further weak Co−Co interactions are present: 3.058(7) and 3.249(3) Å. Average (including all Co−Co contacts): 2.674(16) Å. [f]As found in $[NMe_3(CH_2Ph)]_2[Co_{10}(C_2)(CO)_{21}]$. [g]C−C distance 1.507(13) Å. [h]As found in $[NMe_3(CH_2Ph)]_4[Co_8C(CO)_{17}]$. [i]See reference 3. [j]As found in $[NMe_3(CH_2Ph)]_3[Co_6C(CO)_{12}]\cdot 4CH_3CN$. [k]See reference 2. [l]As found in $[NEt_4][Co_6C(CO)_{14}]$. [m]As found in $[NEt_4]_3[Co_7C(CO)_{15}]$. Only the bonding parameters of the ordered anion are considered. [n]One further weak Co−Co interaction is present: Co(1)−Co(5) 3.089(2) Å. Average (including all Co−Co contacts): 2.653(5) Å.

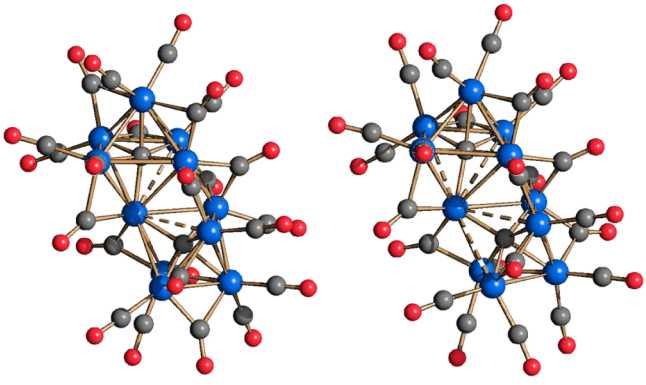

(a) (b)

Figure 8. Molecular structures of (a) $[Co_{11}C_2(CO)_{23}]^-$ and (b) $[Co_{11}C_2(CO)_{23}]^{2-}$ (blue, Co; red, O; gray, C). Co−Co contacts ≤3.02 Å are represented as full lines, while those in the range of 3.02−3.35 Å are depicted as fragmented lines.

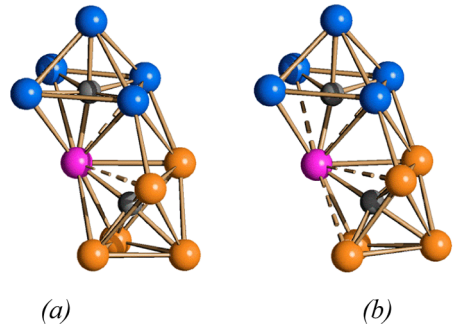

(a) (b)

Figure 9. The $Co_{11}C_2$ metal cage of (a) $[Co_{11}C_2(CO)_{23}]^-$ and (b) $[Co_{11}C_2(CO)_{23}]^{2-}$ showing their origin from two Co_6C octahedrons sharing a common vertex (purple, common vertex; blue and orange are used for the two octahedral units). Co−Co contacts ≤3.02 Å are represented as full lines, while those in the range of 3.02−3.35 Å are depicted as fragmented lines.

$[Co_{11}C_2(CO)_{23}]^-$ (154 CVE) is isoelectronic with $[Co_{11}N_2(CO)_{21}]^{3-}$, but since there is one additional interoctahedra Co−Co bond, we would expect for it only 148 CVE (86 × 2 (Oh) − 18 (vertex) − 2 × 3 (Oh−Oh bonds) = 148 CVE). Thus, because the dicarbide is even more electron-rich than the dinitride, this results in a further elongation of some Co−Co bonds at the point that two of them are at the border between bonding and nonbonding. Similarly, the addition of a further electron in the $[Co_{11}C_2(CO)_{23}]^{2-}$ dianion (155 CVE) causes the weakening of two more bonds as demonstrated by its solid-state structure. This trend might explain the instability of the $[Co_{11}C_2(CO)_{23}]^{3-}$ trianion (156 CVE), which possesses an additional electron.

The Co−$C_{carbide}$ interactions are more spread in the $[Co_{11}C_2(CO)_{23}]^{2-}$ dianion [1.875(9)−2.032(8) Å] than they are in the $[Co_{11}C_2(CO)_{23}]^-$ monoanion [1.874(13)−1.975(13) Å], whereas the average values are almost identical [1.93(3) and 1.94(4) Å, respectively]. These values are slightly longer than those that are usually found for carbides in Co_6C octahedral cavities, for example, $[Co_6C(CO)_{13}]^{2-}$ 1.852(4)−1.880(4) Å, average 1.867(10).[2]

$[Co_{11}C_2(CO)_{23}]^-$ contains 13 terminal and 10 edge-bridging CO ligands, whereas $[Co_{11}C_2(CO)_{23}]^{2-}$ displays 14 terminal and 9 edge-bridging COs. The bent bi-octahedral structures of $[Co_{11}C_2(CO)_{23}]^{n-}$ (n = 1, 2) maintain the two carbide atoms far apart [3.199(16) and 3.163(12) Å, respectively] with very similar $C_{carbide}$−Co_{shared}−$C_{carbide}$ angles [114.3(5) and 111.7(4)°, respectively].

dx.doi.org/10.1021/ic500161e | Inorg. Chem. 2014, 53, 3818−3831

$[Co_{10}(C_2)(CO)_{21}]^{2-}$. Within the crystal, this cluster is located on a 2-fold axis passing through the two interstitial C-atoms, and thus, only half of it is present in the asymmetric unit of the unit cell. As far as we are aware, the metal cage of $[Co_{10}(C_2)(CO)_{21}]^{2-}$ (Figure 10 and Table 2) is unprecedented

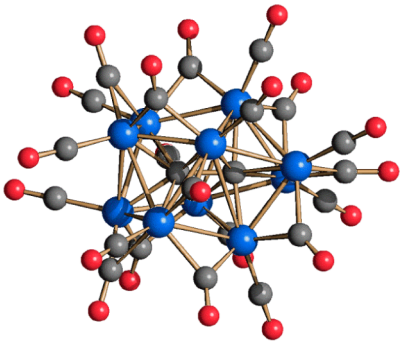

Figure 10. Molecular structure of $[Co_{10}(C_2)(CO)_{21}]^{2-}$ (blue, Co; red, O; gray, C).

in cluster chemistry. This may be viewed as the result of the interpenetration of a Co_8C square antiprismatic framework and a Co_6C octahedral one, sharing four common Co atoms, which describe a distorted butterfly with a missing edge (Figure 11).

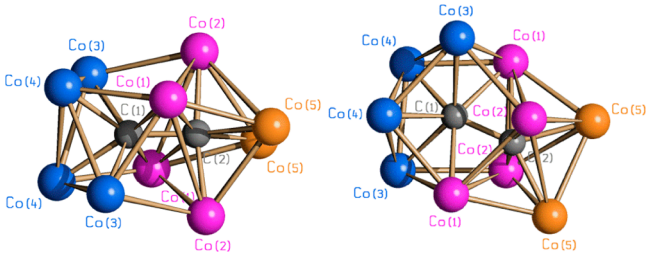

Figure 11. Two views of the $Co_{10}C_2$ metal cage of $[Co_{10}(C_2)(CO)_{21}]^{2-}$, which formally results from the interpenetration of a Co_8C square antiprismatic fragment (blue) and a Co_6C octahedral one (orange) sharing four Co-atoms (purple).

The Co_8C square antiprismatic framework is composed by Co(1), Co(2), Co(3), Co(4), and C(1) (and their symmetry equivalents), whereas the Co_6C octahedron comprises Co(1), Co(2), Co(5), and C(2). As the result of this interpenetration, the two polyhedra are considerably distorted. In particular, one edge on the Co_8C framework [Co(2)···Co(2) 3.797(2) Å] is considerably elongated to accommodate in its center the C(2) atom of the Co_6C octahedron. Thus, the Co_8C framework displays only 15 Co−Co bonding interactions instead of 16, as expected for a regular square antiprism, and 6 $Co-C_{carbide}$ bonds instead of 8 [Co(2)···C(1) 2.513(6) Å]. For comparison, the sum of the covalent radii of Co and C is 1.94 Å.[18] Similarly, the Co_6C octahedron displays 6 $Co-C_{carbide}$ bonds (as expected) but only 11 Co−Co bonds instead of 12, where Co(1)···Co(1) [3.869(2) Å] is the "open edge". As a further result of this interpenetration, the Co−Co bonding interactions are rather spread [2.4691(14)−3.012(2) Å; average 2.623(4) Å].

The $Co-C_{carbide}$ interactions are rather loose [1.9038(12)−2.205(3) Å; average 2.039(15) Å], and this may be accounted for by the following: (1) the presence of very distorted and "stretched" cavities, (2) a large square antiprismatic cavity, and (3) the presence of a direct C−C bond [1.507(13) Å]. In particular, in view of the short C(1)−C(2) distance, the cluster is better described as monoacetylide rather than a dicarbide. Several Co, Ni, and Co−Ni carbonyl clusters containing one or more tightly bonded C_2 units, usually described in the literature as "acetylides," are known, displaying C−C bonds in the range of 1.35−1.54 Å.[21−23]

Finally, the surface of the cluster is decorated by 21 CO ligands, 10 terminal (one per Co-atom), and 11 edge-bridging.

The polyhedral condensation rules[21] predict 138 CVE for a cluster resulting from the condensation of a square antiprism and an octahedron sharing a butterfly (114 (square-antiprism) + 86 (Oh) − 62 (butterfly) = 138 CVE or 140 CVE if we consider that in the butterfly there is a missing edge). Thus, $[Co_{10}(C_2)(CO)_{21}]^{2-}$ (142 CVE) is electron-rich, as often found for polycarbide clusters.

$[Co_8C(CO)_{17}]^{4-}$. The structure of the $[Co_8C(CO)_{17}]^{4-}$ tetra-anion (Figure 12) is closely related to that of the previously

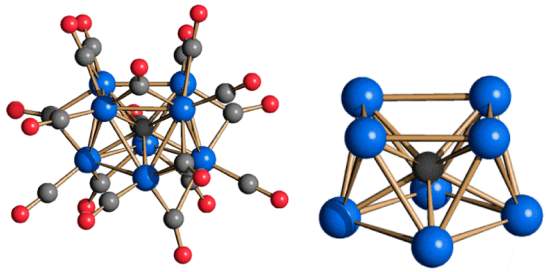

Figure 12. (a) Molecular structure of $[Co_8C(CO)_{17}]^{4-}$ and (b) its Co_8C metal cage (blue, Co; red, O; gray, C).

reported $[Co_8C(CO)_{18}]^{2-}$ dianion.[3] Their metal atom polyhedron can be described as a square antiprism elongated along one of the 2-fold axes, resulting in the idealized D_2 symmetry instead of D_{4d}.

The Co−Co distances in the $[Co_8C(CO)_{17}]^{4-}$ tetra-anion [2.4656(15)−2.6690(15) Å] are more spread than they are in the $[Co_8C(CO)_{18}]^{2-}$ dianion [2.464(2)−2.598(2) Å], even if their average values are almost identical [2.527(6) and 2.52(8) Å, respectively]. Also the $Co-C_{carbide}$ distances are similar in the two clusters, that is, $[Co_8C(CO)_{17}]^{4-}$ 2.012(7)−2.150(7) Å, average 2.07(2) Å; $[Co_8C(CO)_{18}]^{2-}$ 1.95(2)−2.20(2) Å, average 2.07(6) Å. Thus, it seems that the increased negative charge does not affect very much the Co_8C metal cage. Regarding the stereochemistry of the CO ligands, the $[Co_8C(CO)_{17}]^{4-}$ tetra-anion contains eight terminal and nine μ-CO ligands, whereas the $[Co_8C(CO)_{18}]^{2-}$ dianion possesses nine terminal and nine μ-CO ligands. The two clusters are isoelectronic (114 CVE).

$[Co_6C(CO)_{12}]^{3-}$. The asymmetric unit of the unit cell of $[NMe_3(CH_2Ph)]_3[Co_6C(CO)_{12}]\cdot 4CH_3CN$ contains two-sixths of two cluster anions (on $\bar{3}$). The independent parts of the two cluster anions comprise, each, one Co-atom, the carbide, and two CO ligands. The two molecules, generated after applying symmetry operations, are almost identical.

The $[Co_6C(CO)_{12}]^{3-}$ trianion displays a distorted octahedral geometry, with crystallographic $\bar{3}$ (D_{3d}) symmetry (Figure 13). Thus, the cluster is better described as a trigonal antiprism or an octahedron compressed along one of its 3-fold axis. The cluster is completed by 12 carbonyls, six of which are terminal

dx.doi.org/10.1021/ic500161e | Inorg. Chem. 2014, 53, 3818−3831

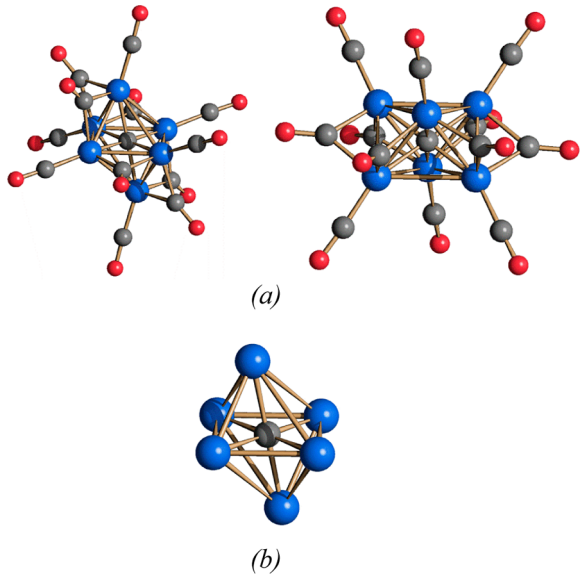

Figure 13. (a) Molecular structure of $[Co_6C(CO)_{12}]^{3-}$ (two views are reported, one showing the octahedral structure and the second showing its D_{3d} symmetry) and (b) its Co_6C metal cage (blue, Co; red, O; gray, C).

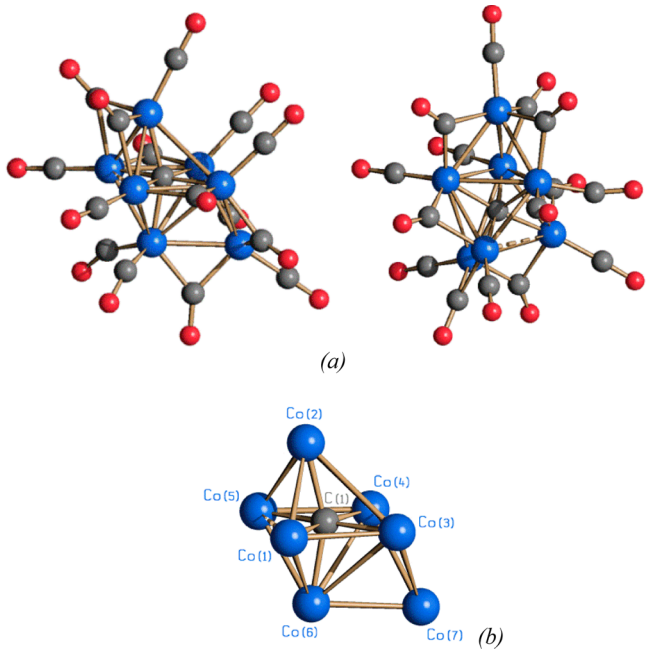

Figure 14. (a) Molecular structure of $[Co_7C(CO)_{15}]^{3-}$ (two views are reported) and (b) its Co_7C metal cage (blue, Co; red, O; gray, C). Co−Co contacts ≤3.02 Å are represented as full lines, Co(1)···Co(5) (3.089(2) Å) as fragmented line.

(one per each Co atom) and six others that are μ-CO, bridging all the six interbasal edges of the trigonal antiprism.

The octahedral geometry has been previously found in two other Co monocarbide carbonyls, that is, $[Co_6C(CO)_{13}]^{2-}$[2] and the paramagnetic $[Co_6C(CO)_{14}]^{-}$.[3] It is interesting that, despite their different charges, electron counts, and number of CO ligands, these three clusters display very similar bonding parameters (Table 2).

With 86 CVE, the $[Co_6C(CO)_{13}]^{2-}$ dianion is electron-precise; however, $[Co_6C(CO)_{12}]^{3-}$ is electron-poor (85 CVE), and $[Co_6C(CO)_{14}]^{-}$ is electron-rich (87 CVE). Both $[Co_6C(CO)_{12}]^{3-}$ and $[Co_6C(CO)_{14}]^{-}$ are paramagnetic because of one unpaired electron, as evidenced by EPR experiments.[3] In theory, an 86 CVE $[Co_6C(CO)_{12}]^{4-}$ might exist, but in view of its very high negative charge, it is probably readily oxidized to the paramagnetic trianion. Even if the free $[Co_6C(CO)_{12}]^{4-}$ tetra-anion has not been observed, some of its derivatives stabilized by Au(I) or Hg(II) fragments have been previously isolated, for example, $[Co_6C(CO)_{12}(AuPPh_3)_2]^{2-}$ and $[Co_6C(CO)_{12}\{\mu_3\text{-}HgW(CO)_3Cp\}_2]^{2-}$.[24,25]

$[Co_7C(CO)_{15}]^{3-}$. Within the asymmetric unit of the unit cell of $[NEt_4]_3[Co_7C(CO)_{15}]$, there are two independent $[Co_7C(CO)_{15}]^{3-}$ anions that display almost identical structures, one ordered and one disordered over two symmetry-related (by 2) positions. For the sake of simplicity, we will use in this discussion only the bonding parameters of the ordered anion (Figure 14). The metal cage of $[Co_7C(CO)_{15}]^{3-}$ may be described as a C-centered distorted octahedron with the seventh Co μ_3-capping a triangular face. The six Co−$C_{carbide}$ contacts [1.870(7)−1.937(7) Å; average 1.895(17) Å] are comparable to those found in other octahedral Co_6C clusters (see Table 2). The cluster displays 15 Co−Co contacts, of which 14 are bonding [2.5022(14)−2.8876(14) Å; average 2.622(5) Å], whereas the Co(1)−Co(5) interaction [3.089(2) Å] may be considered as weakly bonding. The structure is completed by 15 CO ligands, of which 8 are terminal and 7 are edge-bridging.

A μ_3-capped octahedron should possess 98 CVE,[20,26] as found in several M_7C carbide clusters.[27−29] In this respect, $[Co_7C(CO)_{15}]^{3-}$ (100 CVE) is electron-rich, and the current electron-counting rules predict for it a capped trigonal prismatic structure, as found in $[M_7N(CO)_{15}]^{2-}$ (M = Co, Rh),[30] $[Ni_4Os_3C(CO)_{15}]^{2-}$[31], and $[Ni_7C(CO)_{12}]^{2-}$.[21b] Nonetheless, $[Co_7C(CO)_{15}]^{3-}$ adopts a capped octahedral structure, and to accommodate the two extra electrons, some Co−Co bonds are elongated, causing distortions in the metal polyhedron, as noticed above.

3. CONCLUSIONS

The $[Co_6C(CO)_{15}]^{2-}$ monocarbide carbonyl cluster is a very versatile starting material for the preparation of several Co-carbide clusters via thermal or redox reactions (Scheme 2). Its thermal decomposition has been widely explored previously,[2,4,6] whereas a detailed study of its oxidation and reduction reactions has been reported in this Paper for the first time. As a major result of the present study, we have

Scheme 2

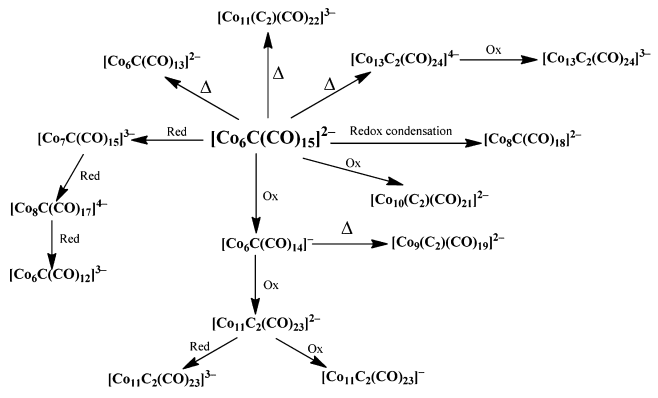

dx.doi.org/10.1021/ic500161e | Inorg. Chem. 2014, 53, 3818−3831

synthesized and fully characterized the new species $[Co_{11}C_2(CO)_{23}]^{2-}$, $[Co_{11}C_2(CO)_{23}]^{-}$, $[Co_{10}(C_2)(CO)_{21}]^{2-}$, $[Co_8C(CO)_{17}]^{4-}$, $[Co_6C(CO)_{12}]^{3-}$, and $[Co_7C(CO)_{15}]^{3-}$.

Overall, the chemistry of Co-carbide carbonyl clusters seems to be very rich, including monocarbide, that is, $[Co_6C(CO)_{15}]^{2-}$,[1] $[Co_6C(CO)_{14}]^{-}$,[3] $[Co_6C(CO)_{13}]^{2-}$,[2] $[Co_6C(CO)_{12}]^{3-}$, $[Co_7C(CO)_{15}]^{3-}$, $[Co_8C(CO)_{18}]^{2-3}$, and $[Co_8C(CO)_{17}]^{4-}$, dicarbide, that is, $[Co_{11}C_2(CO)_{23}]^{n-}$ (n = 1−3) and $[Co_{13}C_2(CO)_{24}]^{n-}$ (n = 3, 4),[4] and monoacetylide species, that is, $[Co_9(C_2)(CO)_{19}]^{2-}$,[5] $[Co_{10}(C_2)(CO)_{21}]^{2-}$, and $[Co_{11}(C_2)(CO)_{22}]^{3-}$.[6] This is due to the stabilizing effect of the interstitial C-atoms, which sometimes leads also to the development in these clusters of electrochemical and/or magnetic properties. Indeed, the previously reported $[Co_{13}C_2(CO)_{24}]^{4-}$ and $[Co_8C(CO)_{18}]^{2-}$ as well as the new $[Co_{11}C_2(CO)_{23}]^{2-}$ clusters display reversible (in the time scale of cyclic voltammetry) redox processes, and in a few cases, differently charged anions are sufficiently stable to be isolated in the solid state, that is, $[Co_{11}C_2(CO)_{23}]^{n-}$ (n = 1, 2) and $[Co_{13}C_2(CO)_{24}]^{n-}$ (n = 3, 4). In addition, the $[Co_6C(CO)_{14}]^{-}$,[3] $[Co_6C(CO)_{12}]^{3-}$, $[Co_9(C_2)(CO)_{19}]^{2-}$,[5] $[Co_{11}C_2(CO)_{23}]^{2-}$, and $[Co_{13}C_2(CO)_{24}]^{4-4}$ odd electron paramagnetic species (S = 1/2) were characterized by means of X-ray crystallography and EPR spectroscopy.

As a general conclusion, despite the fact that $[Co_6C(CO)_{15}]^{2-}$ was isolated several years ago, the chemistry of this dianion has not yet been fully explored, and new results may be obtained using it as precursor for both homo- and bimetallic Co-carbide carbonyl clusters.

4. EXPERIMENTAL SECTION

4.1. General Procedures. All reactions and sample manipulations were carried out using standard Schlenk techniques under nitrogen and in dried solvents. All the reagents were commercial products (Aldrich) of the highest purity available and used as received, except $[NR_4]_2[Co_6C(CO)_{15}]$ and $[NR_4]_2[Co_6C(CO)_{13}]$ ($[NR_4]^+ = [NEt_4]^+$, $[NMe_3(CH_2Ph)]^+$), which were prepared according to the literature.[1,2] Analysis of Co was performed by atomic absorption on a Pye-Unicam instrument. Analyses of C, H, and N were obtained with a Thermo Quest Flash EA 1112NC instrument. IR spectra were recorded on a Perkin-Elmer Spectrum One interferometer in CaF_2 cells. Structure drawings were performed with SCHAKAL99.[32]

The electrochemical experiments were performed with a PGSTAT302N (Autolab) potentiostat equipped with a nitrogen-purged three-electrode cell containing a gold working electrode, an SCE as the reference electrode, and a Pt wire as the counter electrode; $[NBu_4][BF_4]$ 0.1 M was used as supporting electrolyte.

EPR spectra were obtained by using an EPR Varian E 112 instrument, operating at X-band, equipped with an Oxford EPR 900 cryostat for temperature control and with a Bruker ER035 M NMR Gaussmeter and a XL Microwave 3120 frequency counter for a precise g-value determination. The spectrometer was interfaced to an IPC 610/P566C industrial grade Advantech computer through a data acquisition system, which was able to give in real time the average signal,[33] and a software package specially designed for EPR experiments.[34] The optimization of spin-Hamiltonian parameters and the EPR data fitting was accomplished using the Winsim[35] and SIMPOW[36] software packages in the temperature range of 110−296 K.

4.2. Synthesis of $[NMe_3(CH_2Ph)][Co_6C(CO)_{14}]$. $HBF_4{\cdot}Et_2O$ (150 μL, 1.09 mmol) was added in small portions over a period of 2 h to a solution of $[NMe_3(CH_2Ph)]_2[Co_6C(CO)_{15}]$ (1.12 g, 1.04 mmol) in THF (30 mL), and the mixture was stirred at room temperature for 3 h. The solvent was then removed in vacuo; the solid residue was then dissolved in CH_2Cl_2 (20 mL), and the solution was stirred at room temperature overnight. The solvent was then removed in vacuo; the residue was washed with H_2O (40 mL) and toluene (40 mL), and it was extracted in CH_2Cl_2 (20 mL). Slow diffusion of n-hexane (40 mL) afforded X-ray quality single crystals of $[NMe_3(CH_2Ph)][Co_6C(CO)_{14}]$ (yield = 0.76 g, 81% based on Co). $C_{25}H_{16}Co_6NO_{14}$ (907.97): calcd. C 33.05, H 1.78, N 1.54, Co 38.96; found: C 33.22, H 1.74, N 1.31, Co 39.12%. IR (THF, 293 K) ν(CO): 2012(s), 1855(m) cm^{-1}. Note: The $[NEt_4][Co_6C(CO)_{14}]$ salt may be obtained operating as above starting from $[NEt_4]_2[Co_6C(CO)_{15}]$.

4.3. Synthesis of $[NMe_3(CH_2Ph)]_2[Co_{11}C_2(CO)_{23}]$. $HBF_4{\cdot}Et_2O$ (600 μL, 4.36 mmol) was added in small portions over a period of 2 h to a solution of $[NMe_3(CH_2Ph)]_2[Co_6C(CO)_{15}]$ (1.12 g, 1.04 mmol) in THF (30 mL), and the mixture was stirred at room temperature for 3 h. The solvent was then removed in vacuo; the solid residue was then dissolved in CH_2Cl_2 (20 mL), and the solution was stirred at room temperature overnight. The solvent was then removed in vacuo; the residue was washed with H_2O (40 mL) and toluene (40 mL), and it was extracted in CH_2Cl_2 (20 mL). Slow diffusion of n-hexane (40 mL) afforded X-ray quality single crystals of $[NMe_3(CH_2Ph)]_2[Co_{11}C_2(CO)_{23}]$ (yield = 1.14 g, 68% based on Co). $C_{45}H_{32}Co_{11}N_2O_{23}$ (1616.96): calcd. C 33.41, H 2.00, N 1.73, Co 40.10; found: C 33.25, H 2.12, N 1.96, Co 40.38%. IR (nujol, 293 K) ν(CO): 2012(vs), 1852(m) cm^{-1}. IR (CH_2Cl_2, 293 K) ν(CO): 2018(s), 1853 (m) cm^{-1}. IR (THF, 293 K) ν(CO): 2014(s), 1856(m) cm^{-1}. IR (acetone, 293 K) ν(CO): 2014(s), 1840(m) cm^{-1}.

Note: Sometimes some crystals of the solvate $[NMe_3(CH_2Ph)]_2[Co_{11}C_2(CO)_{23}]{\cdot}0.25CH_2Cl_2$ are obtained in mixture with $[NMe_3(CH_2Ph)]_2[Co_{11}C_2(CO)_{23}]$. This contamination is not generally a problem, since the two salts contain the same cluster. In all cases, it may be avoided by crystallizing $[NMe_3(CH_2Ph)]_2[Co_{11}C_2(CO)_{23}]$ from THF/n-hexane. The salts $[NEt_4]_2[Co_{11}C_2(CO)_{23}]$ may be obtained operating as above starting from $[NEt_4]_2[Co_6C(CO)_{15}]$.

4.4. Synthesis of $[NMe_3(CH_2Ph)][Co_{11}C_2(CO)_{23}]$. $HBF_4{\cdot}Et_2O$ (900 μL, 6.54 mmol) was added in small portions over a period of 2 h to a solution of $[NMe_3(CH_2Ph)]_2[Co_6C(CO)_{15}]$ (1.12 g, 1.04 mmol) in THF (30 mL), and the mixture was stirred at room temperature for 3 h. The solvent was then removed in vacuo; the solid residue was dissolved in CH_2Cl_2 (20 mL), and the solution was stirred at room temperature overnight. The solvent was then removed in vacuo; the residue was washed with H_2O (40 mL) and toluene (40 mL), and it was extracted in CH_2Cl_2 (20 mL). Slow diffusion of n-hexane (40 mL) afforded X-ray quality single crystals of $[NMe_3(CH_2Ph)][Co_{11}C_2(CO)_{23}]$ (yield = 0.81 g, 53% based on Co). $C_{35}H_{16}Co_{11}NO_{23}$ (1466.72): calcd. C 28.64, H 1.10, N 0.96, Co 44.21; found: C 28.42, H 0.91, N 1.11, Co 44.38%. IR (nujol, 293 K) ν(CO): 2030(vs), 1874(m) cm^{-1}. IR (CH_2Cl_2, 293 K) ν(CO): 2050(s), 1876 (m) cm^{-1}.

Note: Sometimes some crystals of the solvate $[NMe_3(CH_2Ph)][Co_{11}C_2(CO)_{23}]{\cdot}0.5CH_2Cl_2$ are obtained in mixture with $[NMe_3(CH_2Ph)][Co_{11}C_2(CO)_{23}]$. This contamination is not generally a problem, since the two salts contain the same cluster. In all cases, it may be avoid by crystallizing $[NMe_3(CH_2Ph)][Co_{11}C_2(CO)_{23}]$ from THF and n-hexane.

4.5. Reduction of $[NMe_3(CH_2Ph)]_2[Co_{11}C_2(CO)_{23}]$. Cp_2Co (91.0 mg, 0.481 mmol) was added in small portions over a period of 0.5 h to a solution of $[NMe_3(CH_2Ph)]_2[Co_{11}C_2(CO)_{23}]$ (0.750 g, 0.464 mmol) in THF (15 mL), and the mixture was stirred at room temperature for 1 h. The IR spectrum indicated, at this point, the presence in solution only of a new species tentatively formulated as $[Co_{11}C_2(CO)_{23}]^{3-}$ (ν(CO) 1976 (vs), 1768(m) cm^{-1}). The solvent was then removed in vacuo; the residue was washed with H_2O (40 mL) and toluene (40 mL), and it was extracted in THF (20 mL). Slow diffusion of n-hexane (40 mL) on the THF solution afforded a mixture of crystals of $[Cp_2Co]_2[Co_6C(CO_{15}]$ and $[NMe_3(CH_2Ph)]_2[Co_6C(CO_{15}]$. The same result was obtained also by directly layering n-hexane on the crude THF reaction mixture before workup. This suggests that the purported $[Co_{11}C_2(CO)_{23}]^{3-}$ trianion is not stable enough to allow its isolation in the solid state, and therefore, no further characterization was possible. The tentative formulation of the reduced species as $[Co_{11}C_2(CO)_{23}]^{3-}$ is based on IR and electrochemical data,

dx.doi.org/10.1021/ic500161e | Inorg. Chem. 2014, 53, 3818−3831

Table 3. Crystal Data and Experimental Details of Studied Compounds

	$[NMe_3(CH_2Ph)][Co_6C(CO)_{14}]$	$[NEt_4][Co_6C(CO)_{14}]$	$[NMe_3(CH_2Ph)]_2[Co_{11}C_2(CO)_{23}]$
formula	$C_{25}H_{16}Co_6NO_{14}$	$C_{23}H_{20}Co_6NO_{14}$	$C_{45}H_{32}Co_{11}N_2O_{23}$
Fw	907.97	887.98	1616.96
T, K	293(2)	293(2)	100(2)
λ, Å	0.710 73	0.710 73	0.710 73
crystal system	triclinic	tetragonal	monoclinic
space group	$P\bar{1}$	$P4_322$	$C2/c$
a, Å	8.486(6)	8.6041(3)	21.669(4)
b, Å	13.191(10)	8.6041(3)	11.2475(19)
c, Å	14.670(11)	42.833(3)	43.857(9)
α, deg	98.879(9)	90	90
β, deg	100.701(9)	90	102.462(2)
γ, deg	91.722(9)	90	90
cell volume, Å^3	1591(2)	3171.0(3)	10437(3)
Z	2	4	8
D_c, g cm^{-3}	1.895	1.860	2.058
μ, mm^{-1}	3.121	3.130	3.482
F(000)	894	1756	6376
crystal size, mm	0.23 × 0.16 × 0.12	0.19 × 0.16 × 0.12	0.21 × 0.19 × 0.13
θ limits, deg	1.43−26.00	1.90−26.73	1.90−25.03
index ranges	$-10 \le h \le 10$	$-9 \le h \le 10$	$-22 \le h \le 25$
	$-16 \le k \le 16$	$-6 \le k \le 10$	$-13 \le k \le 9$
	$-18 \le l \le 18$	$-54 \le l \le 53$	$-52 \le l \le 52$
reflections collected	12 730	14 375	23 006
independent reflections	6048 [R_{int} = 0.0393]	3373 [R_{int} = 0.0785]	9099 [R_{int} = 0.0468]
completeness to θ max	96.7%	100.0%	98.4%
data/restraints/parameters	6048/126/415	3373/54/201	9099/150/730
goodness on fit on F^2	0.959	0.977	1.144
R_1 ($I > 2\sigma(I)$)	0.0402	0.0413	0.0666
wR_2 (all data)	0.0785	0.0667	0.1564
largest diff. peak and hole, e Å^{-3}	0.424/−0.430	0.357/−0.350	1.621/−1.013
	$[NMe_3(CH_2Ph)]_2[Co_{11}C_2(CO)_{23}]\cdot 0.25CH_2Cl_2$	$[NEt_4]_2[Co_{11}C_2(CO)_{23}]$	$[NMe_3(CH_2Ph)][Co_{11}C_2(CO)_{23}]$
formula	$C_{45.25}H_{32.5}Cl_{0.5}Co_{11}N_2O_{23}$	$C_{41}H_{40}Co_{11}N_2O_{23}$	$C_{35}H_{16}Co_{11}NO_{23}$
Fw	1638.19	1576.98	1466.72
T, K	295(2)	296(2)	293(2)
λ, Å	0.710 73	0.710 73	0.710 73
crystal system	triclinic	orthorhombic	monoclinic
space group	$P\bar{1}$	$Pca2_1$	$P2_1/c$
a, Å	9.9820(10)	45.530(13)	9.790(3)
b, Å	24.042(2)	9.782(3)	12.275(4)
c, Å	24.415(2)	12.033(3)	37.754(12)
α, deg	106.9450(10)	90	90
β, deg	97.0880(10)	90	90.5687(4)
γ, deg	90.8430(10)	90	90
cell volume, Å^3	5554.2(10)	5359(3)	4537(3)
Z	4	4	4
D_c, g cm^{-3}	1.959	1.954	2.147
μ, mm^{-1}	3.297	3.388	3.993
F(000)	3230	3124	2856
crystal size, mm	0.22 × 0.15 × 0.13	0.16 × 0.13 × 0.12	0.24 × 0.21 × 0.16
θ limits, deg	1.42−26.00	1.91−22.72	1.08−25.03
index ranges	$-12 \le h \le 12$	$-42 \le h \le 49$	$-11 \le h \le 11$
	$-29 \le k \le 29$	$-5 \le k \le 10$	$-14 \le k \le 14$
	$-30 \le l \le 30$	$-11 \le l \le 9$	$-44 \le l \le 44$
reflections collected	57 138	10 395	40 049
independent reflections	21 727 [R_{int} = 0.0645]	5852 [R_{int} = 0.1167]	7977 [R_{int} = 0.0614]
completeness to θ max	99.4%	96.0%	99.2%
data/restraints/parameters	21727/543/1471	5852/576/683	7977/153/670
goodness on fit on F^2	0.970	1.010	1.033
R_1 ($I > 2\sigma(I)$)	0.0474	0.0869	0.0822
wR_2 (all data)	0.1027	0.2467	0.2494
largest diff. peak and hole, e Å^{-3}	0.736/−0.461	1.186/−1.077	1.191/−0.953

dx.doi.org/10.1021/ic500161e | Inorg. Chem. 2014, 53, 3818−3831

Table 3. continued

formula	$[NMe_3(CH_2Ph)][Co_{11}C_2(CO)_{23}]\cdot 0.5CH_2Cl_2$ $C_{35.5}H_{17}ClCo_{11}NO_{23}$	$[Cp_2Co]_2[Co_6C(CO_{15}]$ $C_{36}H_{20}Co_8O_{15}$	$[NMe_3(CH_2Ph)]_2[Co_{10}(C_2)(CO)_{21}]$ $C_{43}H_{32}Co_{10}N_2O_{21}$
Fw	1509.18	1163.96	1502.01
T, K	295(2)	295(2)	293(2)
λ, Å	0.710 73	0.710 73	0.710 73
crystal system	triclinic	monoclinic	monoclinic
space group	$P\bar{1}$	$P2/n$	$C2/c$
a, Å	11.6783(7)	10.0609(14)	12.2252(14)
b, Å	14.6091(9)	11.8203(17)	17.194(2)
c, Å	15.2432(16)	17.039(2)	23.594(3)
α, deg	102.6090(10)	90	90
β, deg	95.4510(10)	105.387(2)	91.8730(10)
γ, deg	110.2430(10)	90	90
cell volume, Å^3	2339.5(3)	1953.7(5)	4957.0(10)
Z	2	2	4
D_c, g cm^{-3}	2.142	1.979	2.013
μ, mm^{-1}	3.930	3.378	3.336
F(000)	1470	1144	2968
crystal size, mm	0.19 × 0.16 × 0.12	0.18 × 0.16 × 0.13	0.22 × 0.18 × 0.12
θ limits, deg	1.39−25.03	1.72−25.03	1.73−26.00
index ranges	$-13 \le h \le 13$	$-11 \le h \le 11$	$-15 \le h \le 15$
	$-17 \le k \le 17$	$-14 \le k \le 14$	$-21 \le k \le 21$
	$-18 \le l \le 18$	$-20 \le l \le 20$	$-29 \le l \le 29$
reflections collected	22 545	15 918	25 199
independent reflections	8209 [R_{int} = 0.0225]	3448 [R_{int} = 0.0343]	4849 [R_{int} = 0.0484]
completeness to θ max	99.4%	99.8%	99.9%
data/restraints/parameters	8209/280/565	3448/96/268	4849/48/345
goodness on fit on F^2	1.023	1.062	1.151
R_1 ($I > 2\sigma(I)$)	0.0686	0.0332	0.0569
wR_2 (all data)	0.2249	0.0920	0.1601
largest diff. peak and hole, e Å^{-3}	2.363/−0.815	0.474/−0.477	2.623/−1.055

formula	$[NEt_4]_3[Co_{11}(C_2)(CO)_{22}]\cdot 2CH_3COCH_3$ $C_{54}H_{72}Co_{11}N_3O_{24}$	$[NMe_3(CH_2Ph)]_4[Co_8C(CO)_{17}]$ $C_{58}H_{64}Co_8N_4O_{17}$	$[NMe_3(CH_2Ph)]_3[Co_6C(CO)_{12}]\cdot 4CH_3CN$ $C_{51}H_{60}Co_6N_7O_{12}$	$[NEt_4]_3[Co_7C(CO)_{15}]$ $C_{40}H_{60}Co_7N_3O_{15}$
Fw	1795.38	1560.57	1316.64	1235.42
T, K	100(2)	289(2)	294(2)	293(2)
λ, Å	0.710 73	0.710 73	0.710 73	0.710 73
crystal system	orthorhombic	monoclinic	rhombohedral	monoclinic
space group	*Pcca*	$P2_1/c$	$R\bar{3}$	$C2/c$
a, Å	41.486(3)	14.6212(11)	20.694(15)	40.110(3)
b, Å	15.5536(11)	17.7645(13)	20.694(15)	11.7289(7)
c, Å	20.7702(14)	24.2184(17)	23.638(17)	33.545(2)
α, deg	90	90	90	90
β, deg	90	93.5740(10)	90	109.8090(10)
γ, deg	90	90	120	90
cell volume, Å^3	13 402.0(16)	6278.2(8)	8767(11)	14 847.1(16)
Z	8	4	6	12
D_c, g cm^{-3}	1.780	1.651	1.496	1.658
μ, mm^{-1}	2.723	2.129	1.725	2.353
F(000)	7248	3168	4038	7560
crystal size, mm	0.16 × 0.14 × 0.10	0.24 × 0.21 × 0.16	0.21 × 0.20 × 0.16	0.19 × 0.13 × 0.12
θ limits, deg	1.64−26.00	1.42−26.00	1.43−26.00	1.08−26.00
index ranges	$-51 \le h \le 51$	$-18 \le h \le 18$	$-25 \le h \le 25$	$-49 \le h \le 49$
	$-19 \le k \le 19$	$-21 \le k \le 21$	$-25 \le k \le 25$	$-14 \le k \le 14$
	$-25 \le l \le 25$	$-29 \le l \le 29$	$-29 \le l \le 29$	$-41 \le l \le 41$
reflections collected	132 780	63 908	30 397	75 353
independent reflections	13 155 [R_{int} = 0.1076]	12 310 [R_{int} = 0.0710]	3836 [R_{int} = 0.0376]	14 596 [R_{int} = 0.0626]
completeness to θ max	100.0%	100.0%	100.0%	100.0%
data/restraints/parameters	13 155/558/939	12 310/448/784	3836/110/233	14 596/597/960
goodness on fit on F^2	1.153	1.011	1.063	1.022
R_1 ($I > 2\sigma(I)$)	0.0558	0.0722	0.0291	0.0738
wR_2 (all data)	0.1493	0.2315	0.0782	0.2419
largest diff. peak and hole, e Å^{-3}	1.083/−0.652	1.917/−0.591	0.366/−0.311	1.640/−0.737

dx.doi.org/10.1021/ic500161e | *Inorg. Chem.* 2014, 53, 3818−3831

that is, the reversibility of the first reduction process of $[Co_{11}C_2(CO)_{23}]^{2-}$.

4.6. Synthesis of $[NMe_3(CH_2Ph)]_2[Co_{10}(C_2)(CO)_{21}]$. $[C_7H_7][BF_4]$ (1.02 g, 5.73 mmol) was added in small portions over a period of 4 h to a solution of $[NMe_3(CH_2Ph)]_2[Co_6C(CO)_{15}]$ (1.12 g, 1.04 mmol) in THF (30 mL), and the mixture was stirred at room temperature for 3 h. The solvent was then removed in vacuo; the residue was washed with H_2O (40 mL) and toluene (40 mL), and it was extracted in CH_2Cl_2 (20 mL). Slow diffusion of *n*-hexane (50 mL) afforded a mixture of crystals of $[NMe_3(CH_2Ph)]_2[Co_{11}C_2(CO)_{23}]$ (major product) and $[NMe_3(CH_2Ph)]_2[Co_{10}(C_2)(CO)_{21}]$ (minor product). A few crystals of the latter were mechanically separated to carry out X-ray and spectroscopic analyses. No further characterization was possible. IR (nujol, 293 K) ν(CO): 1997(vs), 1976(m), 1957(sh), 1935(m), 1887(m), 1844(ms), 1879(m) cm^{-1}. IR (CH_2Cl_2, 293 K) ν(CO): 2010(vs), 1833(ms) (m) cm^{-1}. IR (THF, 293 K) ν(CO): 2007(vs), 1837(ms) cm^{-1}. IR (acetone, 293 K) ν(CO): 2007(vs), 1832(ms) cm^{-1}. IR (CH_3CN, 293 K) ν(CO): 2005(vs), 1828(ms) cm^{-1}.

4.7. Synthesis of $[NEt_4]_3[Co_7C(CO)_{15}]$. A solution of Na/naphthalene in THF was added in small portions over a period of 4 h to a solution of $[NEt_4]_2[Co_6C(CO)_{15}]$ (1.12 g, 1.12 mmol) in THF (30 mL), and the reaction was monitored via IR spectroscopy after each addition. A precipitate started to form, and when (by IR) the solution contained a mixture of $[Co(CO)_4]^-$ (major) and $[Co_6C(CO)_{13}]^{2-}$ (minor) anions, the solvent was removed in vacuo. The residue was then dissolved in DMF (15 mL), and the crude mixture was precipitated by adding a saturated solution of $[NEt_4]Br$ in H_2O (40 mL). The solid was recovered by filtration and washed with H_2O (40 mL), toluene (20 mL), THF (20 mL), and acetone (20 mL). The trianion $[Co_7C(CO)_{15}]^{3-}$ was finally extracted in CH_3CN, and crystals of $[NEt_4]_3[Co_7C(CO)_{15}]$ were obtained after slow diffusion of *n*-hexane (5 mL) and diisopropyl ether (40 mL) into the CH_3CN solution (yield = 0.23 g, 19% based on Co). Even if the yield is low, the compound was obtained in a highly pure crystalline form after workup. $C_{40}H_{60}Co_7N_3O_{15}$ (1235.45): calcd. C 38.87, H 4.90, N 3.40, Co 33.41; found: C 39.11, H 4.71, N 3.65, Co 33.23%. IR (CH_3CN, 293 K) ν(CO): 1943(s), 1770 (m) cm^{-1}.

4.8. Synthesis of $[NMe_3(CH_2Ph)]_4[Co_8C(CO)_{17}]$. A solution of Na/naphthalene in THF was added in small portions over a period of 4 h to a solution of $[NMe_3(CH_2Ph)]_2[Co_6C(CO)_{15}]$ (1.12 g, 1.04 mmol) in THF (30 mL), and the reaction was monitored via IR spectroscopy after each addition. A precipitate started to form, and when (by IR) the solution contained only $[Co(CO)_4]^-$, the solvent was removed in vacuo. This requires a greater amount of reducing agent than the synthesis of $[NEt_4]_3[Co_7C(CO)_{15}]$ requires. The residue was, then, dissolved in DMF (15 mL), and the crude mixture was precipitated by adding a saturated solution of $[NMe_3(CH_2Ph)]Cl$ in H_2O (40 mL). The solid was recovered by filtration and washed with H_2O (40 mL), toluene (20 mL), THF (20 mL) (containing some unreacted $[Co_6C(CO)_{15}]^{2-}$), and acetone (20 mL) (containing some $[Co_7C(CO)_{15}]^{3-}$). The tetra-anion $[Co_8C(CO)_{17}]^{4-}$ was finally extracted in CH_3CN, and crystals suitable for X-ray analysis of $[NMe_3(CH_2Ph)]_4[Co_8C(CO)_{17}]$ were obtained after slow diffusion of *n*-hexane (5 mL) and diisopropyl ether (40 mL) into the CH_3CN solution (yield = 0.23 g, 19% based on Co). Even if the yield is low, the compound was obtained in a highly pure crystalline form after workup. $C_{58}H_{64}Co_8N_4O_{17}$ (1560.57): calcd. C 44.62, H 4.13, N 3.59, Co 30.22; found: C 44.41, H 4.43, N 3.91, Co 29.95%. IR (nujol, 293 K) ν(CO): 1976(sh), 1923(m), 1901(vs), 1860(m), 1742(sh), 1711(ms) cm^{-1}. IR (CH_3CN, 293 K) ν(CO): 1922(s), 1744 (m) cm^{-1}.

4.9. Synthesis of $[NMe_3(CH_2Ph)]_3[Co_6C(CO)_{12}]\cdot 4CH_3CN$. A solution of Na/naphthalene in THF was added in small portions over a period of 4 h to a solution of $[NMe_3(CH_2Ph)]_2[Co_6C(CO)_{15}]$ (1.12 g, 1.04 mmol) in THF (30 mL), and the reaction was monitored via IR spectroscopy after each addition. A precipitate started to form, and when (by IR) the solution contained only $[Co(CO)_4]^-$, further Na/naphthalene was added before removing the solvent in vacuo. The residue was then dissolved in DMF (15 mL), and the crude mixture was precipitated by adding a saturated solution of $[NMe_3(CH_2Ph)]Cl$ in H_2O (40 mL). The solid was recovered by filtration and washed with H_2O (40 mL), toluene (20 mL), THF (20 mL), and acetone (20 mL). The trianion $[Co_6C(CO)_{12}]^{3-}$ was finally extracted in CH_3CN, and crystals suitable for X-ray analysis of $[NMe_3(CH_2Ph)]_3[Co_6C(CO)_{12}]\cdot 4CH_3CN$ were obtained after slow diffusion of *n*-hexane (5 mL) and diisopropyl ether (40 mL) into the CH_3CN solution (yield = 0.28 g, 20% based on Co). Even if the yield is low, the compound was obtained in a highly pure crystalline form after workup. $C_{51}H_{60}Co_6N_7O_{12}$ (1316.64): calcd. C 46.50, H 4.59, N 7.44, Co 26.87; found: C 46.86, H 4.21, N 7.57, Co 27.11%. IR (nujol, 293 K) ν(CO): 1961(h), 1884(vs), 1871(vs), 1766(ms), 1749(sh), 1735(w) cm^{-1}. IR (CH_3CN, 293 K) ν(CO): 1911(s), 1769 (m) cm^{-1}.

4.10. X-ray Crystallographic Study. Crystal data and collection details for $[NMe_3(CH_2Ph)][Co_6C(CO)_{14}]$, $[NEt_4][Co_6C(CO)_{14}]$, $[NMe_3(CH_2Ph)]_2[Co_{11}C_2(CO)_{23}]$, $[NMe_3(CH_2Ph)]_2[Co_{11}C_2(CO)_{23}]\cdot 0.25CH_2Cl_2$, $[NEt_4]_2[Co_{11}C_2(CO)_{23}]$, $[NMe_3(CH_2Ph)][Co_{11}C_2(CO)_{23}]$, $[NMe_3(CH_2Ph)][Co_{11}C_2(CO)_{23}]\cdot 0.5CH_2Cl_2$, $[Cp_2Co]_2[Co_6C(CO_{15}]$, $[NMe_3(CH_2Ph)]_2[Co_{10}(C_2)(CO)_{21}]$, $[NEt_4]_3[Co_{11}(C_2)(CO)_{22}]\cdot 2CH_3COCH_3$, $[NMe_3(CH_2Ph)]_4[Co_8C(CO)_{17}]$, $[NMe_3(CH_2Ph)]_3[Co_6C(CO)_{12}]\cdot 4CH_3CN$, and $[NEt_4]_3[Co_7C(CO)_{15}]$ are reported in Table 3. The diffraction experiments were carried out on a Bruker APEX II diffractometer equipped with a CCD detector using Mo Kα radiation. Data were corrected for Lorentz polarization and absorption effects (empirical absorption correction SADABS).[37] Structures were solved by direct methods and refined by full-matrix least-squares based on all data using F^2.[38] Hydrogen atoms were fixed at calculated positions and refined by a riding model. All non-hydrogen atoms were refined with anisotropic displacement parameters, unless otherwise stated.

$[NMe_3(CH_2Ph)][Co_6C(CO)_{14}]$. The asymmetric unit of the unit cell contains one cluster anion and one $[NMe_3(CH_2Ph)]^+$ cation (all located on general positions). Similar *U* restraints (s.u. 0.01) were applied to the C and O atoms.

$[NEt_4][Co_6C(CO)_{14}]$. The asymmetric unit of the unit cell contains one-half of a cluster anion and one-half of a $[NMe_3(CH_2Ph)]^+$ cation (all located on 2-fold axes). Similar *U* restraints (s.u. 0.01) were applied to the C and O atoms.

$[NMe_3(CH_2Ph)]_2[Co_{11}C_2(CO)_{23}]$. The asymmetric unit of the unit cell contains one cluster anion and two $[NMe_3(CH_2Ph)]^+$ cations (all located on general positions). Similar *U* restraints (s.u. 0.01) were applied to the C and O atoms.

$[NMe_3(CH_2Ph)]_2[Co_{11}C_2(CO)_{23}]\cdot 0.25CH_2Cl_2$. The asymmetric unit of the unit cell contains two cluster anions (located on general positions), four $[NMe_3(CH_2Ph)]^+$ cations (located on general positions), and one-half (close to an inversion center) of CH_2Cl_2. The half CH_2Cl_2 molecule is disordered over two symmetry-related (by an inversion center) positions; therefore, the independent image has been refined isotropically with 0.5 occupancy factor. Similar *U* restraints were applied to the C and O atoms of the cluster (s.u. 0.01) and to the C and N atoms of the cation (s.u. 0.005). Restraints to bond distances were applied as follows (s.u. 0.01): 1.75 Å for C−Cl in CH_2Cl_2.

$[NEt_4]_2[Co_{11}C_2(CO)_{23}]$. The asymmetric unit of the unit cell contains one cluster anion and two $[NEt_4]^+$ cations (all located on general positions). One of the two cations is disordered, and therefore it has been split into two positions and refined isotropically using one occupancy parameter per disordered group. The crystal is racemically twinned with a refined Flack parameter of 0.41(7),[39] and it was therefore refined using the TWIN refinement routine of SHELXTL. The compound gives rise to very small and low-quality crystals, and therefore, the data were cut at $2\theta = 45.44°$. The cluster anion displays the same structure as that found in $[NMe_3(CH_2Ph)]_2[Co_{11}C_2(CO)_{23}]$ and in $[NMe_3(CH_2Ph)]_2[Co_{11}C_2(CO)_{23}]\cdot 0.25CH_2Cl_2$, and therefore, the data of $[NEt_4]_2[Co_{11}C_2(CO)_{23}]$ were included only for the sake of completeness. Similar *U* restraints (s.u. 0.005) were applied to the C atoms. All the C and O atoms were restrained to isotropic behavior (ISOR line in SHELXL, s.u. 0.01). Restraints to bond distances were applied as follows (s.u. 0.01): 1.47 Å for C−N and 1.53 Å for C−C in $[NEt_4]^+$.

dx.doi.org/10.1021/ic500161e | *Inorg. Chem.* 2014, 53, 3818−3831

$[NMe_3(CH_2Ph)][Co_{11}C_2(CO)_{23}]$. The asymmetric unit of the unit cell contains one cluster anion and one $[NMe_3(CH_2Ph)]^+$ cation (all located on general positions). The crystals appear to be twinned with twin matrix (−1 0 0 0 −1 0 0 0 1) and refined batch scale factor (BASF) 0.1209(15). Similar *U* restraints (s.u. 0.01) were applied to the C and O atoms. The O-atoms of some CO ligands in the cluster anion were restrained to isotropic behavior (ISOR line in SHELXL, s.u. 0.01). Two carbonyl ligands in the anion were disordered, and therefore they were split into two positions each and refined isotropically using one occupancy parameter per disordered group.

$[NMe_3(CH_2Ph)][Co_{11}C_2(CO)_{23}]\cdot 0.5CH_2Cl_2$. The asymmetric unit of the unit cell contains one cluster anion (on a general position), two halves of two $[NMe_3(CH_2Ph)]^+$ cations, and half of a CH_2Cl_2 molecule (close to inversion centers). Similar *U* restraints (s.u. 0.005) were applied to the C and O atoms. Most of the atoms of the CO ligands in the cluster anion were restrained to isotropic behavior (ISOR line in SHELXL, s.u. 0.01). One carbonyl ligand in the anion is disordered, and therefore it was split into two positions and refined isotropically using one occupancy parameter per disordered group. The two halves of the $[NMe_3(CH_2Ph)]^+$ cation are each disordered over two symmetry-related (by an inversion center) positions with the same occupancy factors. The disorder model involves also the half CH_2Cl_2 molecule. Thus, PART −1 of the model includes the first half independent cation (occupancy factor 0.5), whereas PART −2 includes the second half independent cation and the half CH_2Cl_2 molecule (occupancy factors 0.5). Similar *U* restraints (s.u. 0.005) were applied to the C and N atoms of the cations. Restraints to bond distances were applied as follows (s.u. 0.01): 1.75 Å for C−Cl in CH_2Cl_2.

$[Cp_2Co]_2[Co_6C(CO_{15}]$. The asymmetric unit of the unit cell contains half of a cluster anion (on a 2-fold axis) and one $[Cp_2Co]^+$ cation (on a general position). Similar *U* restraints (s.u. 0.01) were applied to the C atoms.

$[NMe_3(CH_2Ph)]_2[Co_{10}(C_2)(CO)_{21}]$. The asymmetric unit of the unit cell contains half of a cluster anion (on a 2-fold axis) and one $[NMe_3(CH_2Ph)]^+$ cation (on a general position). Similar *U* restraints (s.u. 0.01) were applied to the C and O atoms.

$[NEt_4]_3[Co_{11}C_2(CO)_{22}]\cdot 2CH_3COCH_3$. The asymmetric unit of the unit cell contains one cluster anion (on a general position), one full (on a general position) and four halves of $[NEt_4]^+$ cations (on 2-fold axes), and two CH_3COCH_3 molecules (on general positions). Three of the four halves of the $[NEt_4]^+$ cation are disordered over symmetry-related (by 2) positions. Similar *U* restraints (s.u. 0.01) were applied to the C and O atoms. Restraints to bond distances were applied as follows (s.u. 0.01): 1.47 Å for C−N and 1.53 Å for C−C in $[NEt_4]^+$; 1.21 Å for C−O and 1.51 Å for C−C in CH_3COCH_3.

$[NMe_3(CH_2Ph)]_4[Co_8C(CO)_{17}]$. The asymmetric unit of the unit cell contains one cluster anion and four $[NMe_3(CH_2Ph)]^+$ cations (all located on general positions). Similar *U* restraints (s.u. 0.01) were applied to the C and O atoms.

$[NMe_3(CH_2Ph)]_3[Co_6C(CO)_{12}]\cdot 4CH_3CN$. The asymmetric unit of the unit cell contains two-sixths of two cluster anions (on $\bar{3}$), one $[NMe_3(CH_2Ph)]^+$ cation (on a general position), one CH_3CN (on a general position), and one-third of a CH_3CN molecule disordered over three equally populated symmetry-related (by a 3-fold axis) positions. After applying the symmetry operations of the space group, a cation/cluster/CH_3CN ratio of 3:1:4 results. The independent parts of the two cluster anions comprise, each, one Co-atom, the carbide, and two CO ligands. Similar *U* restraints (s.u. 0.01) were applied to the C and O atoms. Restraints to bond distances were applied to the disordered CH_3CN molecule (s.u. 0.01): 1.14 Å for C−N and 1.51 Å for C−C.

$[NEt_4]_3[Co_7C(CO)_{15}]$. The asymmetric unit of the unit cell contains one cluster anion (located on a general position) and half of a cluster anion disordered over two equally populated positions related by an inversion center, four $[NEt_4]^+$ cations (all located on general positions), and half of a $[NEt_4]^+$ cation (located on 2). Some of the C and O atoms of the ordered anion, all the C and O atoms of the disordered anion, and the C atoms of the cations were restrained to isotropic behavior (ISOR line in SHELXL, s.u. 0.01). Similar *U* restraints (s.u. 0.01) were applied to the disordered anion and to all the $[NEt_4]^+$ cations. Restraints to bond distances were applied as follows (s.u. 0.02): 1.47 Å for C−N and 1.53 Å for C−C in $[NEt_4]^+$; 1.16 Å for C−O in the disordered anion.

4.11. DFT Calculations on $[Co_{11}C_2(CO)_{23}]^{2-}$ and $[Co_6C(CO)_{12}]^{3-}$. DFT geometry optimizations and calculation of the electron spin density distributions were performed by the parallel Linux version of the Spartan 10 software.[40] We adopted the B3LYP (Becke, three-parameter, Lee−Yang−Parr)[41,42] exchange-correlation functional formulated with the Becke 88 exchange functional,[43] the correlation functional of Lee, Yang, and Parr,[44] and the 6-31G** base functions set, which is appropriate for calculations of split-valence plus-polarization quality.

■ ASSOCIATED CONTENT

Supporting Information

CIF files giving X-ray crystallographic data for the structure determination of $[NMe_3(CH_2Ph)][Co_6C(CO)_{14}]$, $[NEt_4][Co_6C(CO)_{14}]$, $[NMe_3(CH_2Ph)]_2[Co_{11}C_2(CO)_{23}]$, $[NMe_3(CH_2Ph)]_2[Co_{11}C_2(CO)_{23}]\cdot 0.25CH_2Cl_2$, $[NEt_4]_2[Co_{11}C_2(CO)_{23}]$, $[NMe_3(CH_2Ph)][Co_{11}C_2(CO)_{23}]$, $[NMe_3(CH_2Ph)][Co_{11}C_2(CO)_{23}]\cdot 0.5CH_2Cl_2$, $[Cp_2Co]_2[Co_6C(CO_{15}]$, $[NMe_3(CH_2Ph)]_2[Co_{10}(C_2)(CO)_{21}]$, $[NEt_4]_3[Co_{11}(C_2)(CO)_{22}]\cdot 2CH_3COCH_3$, $[NMe_3(CH_2Ph)]_4[Co_8C(CO)_{17}]$, $[NMe_3(CH_2Ph)]_3[Co_6C(CO)_{12}]\cdot 4CH_3CN$, and $[NEt_4]_3[Co_7C(CO)_{15}]$. This material is available free of charge via the Internet at http://pubs.acs.org.

■ AUTHOR INFORMATION

Corresponding Author

*E-mail: stefano.zacchini@unibo.it. Fax: +39 0512093690.

Notes

The authors declare no competing financial interest.

■ ACKNOWLEDGMENTS

Funding by Fondazione CARIPLO, Project No. 2011-0289, is heartily acknowledged. The University of Bologna is acknowledged for financial support to this work (FARB—Linea d'Intervento 2, "Catalytic transformation of biomass-derived materials into high added-value chemicals," 2014−2016).

■ REFERENCES

(1) (a) Albano, V. G.; Chini, P.; Martinengo, S.; Sansoni, M.; Strumolo, D. *J. Chem. Soc., Chem. Commun.* **1974**, 299. (b) Martinengo, S.; Strumolo, D.; Chini, P.; Albano, V. G.; Braga, D. *J. Chem. Soc., Dalton Trans.* **1985**, 35.

(2) (a) Albano, V. G.; Braga, D.; Martinengo, S. *J. Chem. Soc., Dalton Trans.* **1986**, 981. (b) Albano, V. G.; Chini, P.; Ciani, G.; Sansoni, M.; Strumolo, D.; Heaton, B. T.; Martinengo, S. *J. Am. Chem. Soc.* **1976**, *98*, 5027.

(3) (a) Albano, V. G.; Chini, P.; Ciani, G.; Martinengo, S.; Sansoni, M. *J. Chem. Soc., Dalton Trans.* **1978**, 468. (b) Albano, V. G.; Chini, P.; Ciani, G.; Sansoni, M.; Martinengo, S. *J. Chem. Soc., Dalton Trans.* **1980**, 163.

(4) (a) Albano, V. G.; Braga, D.; Chini, P.; Ciani, G.; Martinengo, S. *J. Chem. Soc., Dalton Trans.* **1982**, 645. (b) Albano, V. G.; Braga, D.; Fumagalli, A.; Martinengo, S. *J. Chem. Soc., Dalton Trans.* **1985**, 1137. (c) Fumagalli, A.; Costa, M.; Della Pergola, R.; Zanello, P.; Fabrizi de Biani, F.; Macchi, P.; Sironi, A. *Inorg. Chim. Acta* **2003**, *350*, 187.

(5) Martinengo, S.; Noziglia, L.; Fumagalli, A.; Albano, V. G.; Braga, D.; Grepioni, F. *J. Chem. Soc., Dalton Trans.* **1998**, 2493.

(6) Albano, V. G.; Braga, D.; Ciani, G.; Martinengo, S. *J. Organomet. Chem.* **1982**, *213*, 293.

(7) *ASM Handbook*, Alloy Phase Diagrams; ASM International: Materials Park, OH, 1992; Vol. 3, p 2.109.

(8) Johnson, B. F. G.; Martin, C. M. In *Metal Clusters in Chemistry;* Braunstein, P., Oro, L. A., Raithby, P. R., Eds.; Wiley-VCH: Weinheim, Germany, 1999, p 877.
(9) Albano, V. G.; Chini, P.; Scatturin, V. *J. Organomet. Chem.* **1968**, *15*, 423.
(10) Zacchini, S. *Eur. J. Inorg. Chem.* **2011**, 4125.
(11) (a) Trimm, D. L. *Catal. Rev.* **1977**, *16*, 155. (b) Rostrup-Nielsen, J.; Trimm, D. L. *J. Catal.* **1977**, *48*, 155. (c) Trimm, D. L. *Catal. Today* **1999**, *49*, 3. (d) Lobo, L. S.; Trimm, D. L. *J. Catal.* **1973**, *29*, 15. (e) Derbyshire, F. J.; Presland, A. E. B.; Trimm, D. L. *Carbon* **1975**, *13*, 111.
(12) (a) Scott, C. D.; Arepalli, S.; Nikolaev, P.; Smalley, R. E. *Appl. Phys. A* **2001**, *72*, 573. (b) Vinciguerra, V.; Buonocore, F.; Panzera, G.; Occhipinti, L. *Nanotechnology* **2003**, *14*, 655. (c) Little, R. B. *J. Cluster Sci.* **2003**, *14*, 135.
(13) (a) Moors, M.; Amara, H.; de Bocarmé, T. V.; Bichara, C.; Ducastelle, F.; Krause, N.; Chalier, J. C. *ACS Nano* **2009**, *3*, 511. (b) Lahiri, J.; Miller, T.; Adamska, L.; Oleynik, I. I.; Batzill, M. *Nano Lett.* **2011**, *11*, 518. (c) Klink, C.; Stensgaard, I.; Besenbacher, F.; Laegsgaard, E. *Surf. Sci.* **1995**, *342*, 250.
(14) Zanello, P. In *Stereochemistry of Organometallic and Inorganic Compounds 5: Chains, Clusters, Inclusion Compounds, Paramagnetic Labels, and Organic Rings;* Zanello, P., Ed.; Elsevier: Amsterdam, London, New York, Tokyo, 1994, p 163.
(15) Connelly, N. G.; Geiger, W. E. *Chem. Rev.* **1996**, 877.
(16) (a) Hieber, W.; Sedlmeier, J. *Ber. Bunsen-Ges.* **1954**, *87*, 25. (b) Behrens, H.; Wakamatsu, H. *Ber. Bunsen-Ges.* **1966**, *99*, 2753. (c) Edgell, W. F.; Lyford, J.; Barbetta, A.; Jose, C. I. *J. Am. Chem. Soc.* **1971**, *93*, 6403.
(17) Bochmann, M. *Organometallics 1;* Oxford Science Publication: England, 1994.
(18) (a) Cordero, B.; Gómez, V.; Platero-Prats, A. E.; Revés, M.; Echevarría, J.; Cremades, E.; Barragán, F.; Alvarez, S. *Dalton Trans.* **2008**, 2832. (b) Bondi, A. *J. Phys. Chem.* **1964**, *68*, 441.
(19) Fumagalli, A.; Ulivieri, P.; Costa, M.; Crispu, O.; Della Pergola, R.; Fabrizi de Biani, F.; Laschi, F.; Zanello, P.; Macchi, P.; Sironi, A. *Inorg. Chem.* **2004**, *43*, 2125.
(20) Mingos, D. M. P.; Wales, D. J. *Introduction to Cluster Chemistry;* Prentice Hall: Englewood Cliffs, NJ, 1990.
(21) (a) Ceriotti, A.; Longoni, G.; Resconi, L.; Manassero, M.; Masciocchi, N.; Sansoni, M. *Chem. Commun.* **1985**, 181. (b) Ceriotti, A.; Piro, G.; Longoni, G.; Manassero, M.; Masciocchi, N.; Sansoni, M. *New J. Chem.* **1988**, *12*, 501. (c) Ceriotti, A.; Piro, G.; Longoni, G.; Manassero, M.; Resconi, L.; Masciocchi, N.; Sansoni, M. *Chem. Commun.* **1985**, 1402.
(22) (a) Femoni, C.; Iapalucci, M. C.; Longoni, G.; Zacchini, S. *Dalton Trans.* **2008**, 3157. (b) Femoni, C.; Iapalucci, M. C.; Longoni, G.; Zacchini, S.; Fedi, S.; Fabrizi de Biani, F. *Dalton Trans.* **2012**, *41*, 4649. (c) Arrigoni, A.; Ceriotti, A.; Della Pergola, R.; Longoni, G.; Manassero, M.; Masciocchi, N.; Sansoni, M. *Angew. Chem., Int. Ed.* **1984**, *23*, 322.
(23) (a) Femoni, C.; Iapalucci, M. C.; Longoni, G.; Zacchini, S. *Eur. J. Inorg. Chem.* **2009**, 2487. (b) Bernardi, A.; Femoni, C.; Iapalucci, M. C.; Longoni, G.; Zacchini, S. *Dalton Trans.* **2009**, 4245.
(24) Reina, R.; Riba, O.; Rossell, O.; Seco, M.; de Montauzon, D.; Font-Bardia, M.; Solans, X. *Eur. J. Inorg. Chem.* **2001**, 1243.
(25) Reina, R.; Riba, O.; Rossell, O.; Seco, M.; de Montauzon, D.; Pellinghelli, M. A.; Tiripicchio, A.; Font-Bardia, M.; Solans, X. *J. Chem. Soc., Dalton Trans.* **2000**, 4464.
(26) Mingos, D. M. P.; May, A. S. Chapter 2. In *The Chemistry of Metal Cluster Complexes;* Shriver, D. F., Kaez, H. D., Adams, R. D., Eds.; VCH: New York, 1990.
(27) (a) Adams, R. D.; Captain, B.; Fu, W.; Hall, M. B.; Mason, J.; Smith, M. D.; Webster, C. E. *J. Am. Chem. Soc.* **2004**, *126*, 5253. (b) Beringhelli, T.; D'Alfonso, G.; de Angelis, M.; Ciani, G.; Sironi, A. *J. Organomet. Chem.* **1987**, *322*, C21. (c) Beringhelli. D'Alfonso, G.; Ciani, G.; Sironi, A.; Molinari, H. *J. Chem. Soc., Dalton Trans.* **1998**, 1281.
(28) (a) Simerly, S. W.; Wilson, S. R.; Shapley, J. R. *Inorg. Chem.* **1992**, *31*, 5146. (b) Lewis, J.; Morewood, C. A.; Raithby, P. R.; Ramirez de Arellano, M. C. *J. Chem. Soc., Dalton Trans.* **1997**, 3335.
(29) (a) Adams, R. D.; Captain, B.; Fu, W.; Pellecchia, P. J.; Smith, M. D. *Inorg. Chem.* **2003**, *42*, 2094. (b) Hermans, S.; Khimyak, T.; Johnson, B. F. G. *Dalton Trans.* **2001**, 3259. (c) Hsu, G.; Wilson, S. R.; Shapley, S. R. *Inorg. Chem.* **1996**, *35*, 923.
(30) (a) Ciani, G.; Masciocchi, N.; Sironi, A.; Fumagalli, A.; Martinengo, S. *Inorg. Chem.* **1992**, *31*, 331. (b) Martinengo, S.; Ciani, G.; Sironi, A. *Chem. Commun.* **1984**, 1572.
(31) Karet, G. B.; Espe, R. L.; Stern, C. L.; Shriver, D. F. *Inorg. Chem.* **1992**, *31*, 2658.
(32) Keller, E. *SCHAKAL99;* University of Freiburg: Freiburg im Breisgau, Baden-Wurttemberg, Germany, 1999.
(33) Ambrosetti, R.; Ricci, D. *Rev. Sci. Instrum.* **1991**, *62*, 2281.
(34) Pinzino, C.; Forte, C. *EPR ENDOR;* ICQEM-CNR: Rome, Italy, 1992.
(35) Duling, D. R. *J. Magn. Reson. B* **1994**, *104*, 105.
(36) Nilges, M. *SIMPOW,* Integrated software for simulation of power systems; Illinois ESR Research Center NIH: Champaign, IL, 2006.
(37) Sheldrick, G. M. *SADABS,* Program for empirical absorption correction; University of Göttingen: Gottingen, Germany, 1996.
(38) Sheldrick, G. M. *SHELX97,* Program for crystal structure determination; University of Göttingen: Gottingen, Germany, 1997.
(39) Flack, H. D. *Acta Crystallogr., Sect. A* **1983**, *39*, 876.
(40) *Spartan 10;* Wavefunction, Inc.: Irvine, CA, 2011.
(41) Kim, K.; Jordan, K. D. *J. Phys. Chem.* **1994**, *98*, 10089.
(42) Stephens, P. J.; Devlin, F. J.; Chabalowski, C. F.; Frisch, M. J. *J. Phys. Chem.* **1994**, *98*, 11623.
(43) Becke, A. D. *Phys. Rev. A* **1988**, *38*, 3098.
(44) Lee, C.; Yang, W.; Parr, R. G. *Phys. Rev. B* **1988**, *37*, 785.